

Modelling piles in FEM-Design

Master's thesis in Structural Engineering & Building Technology

MICHELLE SKJÆRLUND FABRIN

OSAMA ALI BEK

MASTER'S THESIS 2018 ACEX30-18-22

Modelling piles in FEM-Design

MICHELLE SKJÆRLUND FABRIN
OSAMA ALI BEK



CHALMERS
UNIVERSITY OF TECHNOLOGY

Department of Architecture and Civil Engineering
Division of Structural Engineering
CHALMERS UNIVERSITY OF TECHNOLOGY
Gothenburg, Sweden 2018

Modelling piles in FEM-Design
MICHELLE SKJÆRLUND FABRIN
OSAMA ALI BEK

© MICHELLE SKJÆRLUND FABRIN, OSAMA ALI BEK, 2018.

Master's Thesis 2018:22
Department of Architecture and Civil Engineering
Division of Structural Engineering
Chalmers University of Technology
SE-412 96 Gothenburg
Telephone +46 31 772 1000

Cover: Pile model performed in FEM-Design version 17.

Printed by Chalmers Reproservice
Gothenburg, Sweden 2017

Modelling piles in FEM-Design

Master's thesis in the Master's programme Structural Engineering & Building Technology

MICHELLE SKJÆRLUND FABRIN

OSAMA ALI BEK

Department of Architecture and Civil Engineering

Division of Structural Engineering

Chalmers University of Technology

ABSTRACT

The software developer company Strusoft released FEM-Design version 17 in January 2018 which includes the new Pile feature. FEM-Design combines structural and geotechnical Finite Element Modelling which makes the software relevant in projects which combines these two engineering fields. This study includes validation and verification of the Pile feature for two studies; load-displacement behaviour and buckling, respectively. The validation of the load-displacement behaviour consists of two cases where the choice of soil model has been varied. The pile load test is compared with investigations based on analyses of pile and soil modelling in FEM-Design. The buckling verification is performed for a case study with a partially embedded pile in water and partly in soil. The critical buckling load and equivalent length have been estimated from relevant analytical methods and compared with results from FEM-Design. The results of the load-displacement analysis show that the pile modelling of FEM-Design is overly simplified to give agreeable output results. The optimising from the linear soil model to the over-consolidated soil model is insufficient since the stiffness in over-consolidated model is not stress-dependent. Furthermore, the soil history and plastic deformation is not included in the over-consolidated soil model. In general, the pile models show much smaller total resistances than the pile load test. The buckling analysis shows that FEM-Design gives reasonable results compared to the analytical methods.

Key words: FEM-Design, pile modelling, geotechnics, over-consolidation, lateral earth pressure coefficient, finite element, Wehnert, compression modulus.

Contents

Abstract	ii
Acknowledgement	v
Notations	vi
1 Introduction	1
1.1 Background	1
1.2 Aim of the Thesis	2
1.3 Objectives	2
1.4 Method	2
1.5 Limitation of the Thesis	3
1.6 Overview	3
2 Modelling piles in FEM-Design	4
2.1 Modelling of the soil	4
2.1.1 Linear soil model	5
2.1.2 Over-consolidated soil model	5
2.2 Soil-pile interaction	7
2.2.1 Support stiffnesses	7
2.2.2 Plastic limit forces	8
2.3 Modelling of the pile	10
2.4 Analyses	11
2.4.1 Linear elastic analysis	12
2.4.2 Non-linear elastic analysis	12
2.4.3 Non-linear plastic analysis	13
2.5 Output results	13
2.5.1 Translational displacement	13
2.5.2 Reactions	14
2.5.3 Internal forces	15
2.6 Limitation of FEM-Design	15
3 Validation of pile load test	17
3.1 Introduction	17
3.2 Background	17
3.3 Modelling the pile in FEM-Design	18
3.4 Case 1 - Linear soil model	19

3.4.1	Introduction	19
3.4.2	Results & discussions	19
3.5	Case 2 - Over-consolidated soil model	23
3.5.1	Introduction	23
3.5.2	Input values	23
3.5.3	Results & Discussions	26
3.6	Sensitivity analysis	29
4	Verification of buckling load of partially embedded pile	31
4.1	Introduction	31
4.2	Estimation of critical buckling load and equivalent length	32
4.2.1	Analytical methods	32
4.2.2	FEM-Design	35
4.3	Case 3 - Partially embedded pile	36
4.4	Results & Discussions	37
5	Conclusion	40
5.1	Conclusion	40
5.2	Recommendations for using FEM-Design	41
5.3	Recommendation for further studies	41
	Bibliography	44
	Appendices	45

Acknowledgement

This Thesis has been carried out during the Spring term 2018 as a collaboration between the Division of Structural Engineering at Chalmers University of Technology and the consultant company Ramböll.

We would like to thank our supervisor Jelke Dijkstra at Chalmers for guidance and contribution to our project; both the supervision regarding theory of geotechnics and practical questions for the report.

The work of the Thesis has been a cooperation with Ramböll where we would like to thank Rikard Möse for the supervision. We want to acknowledge the Port & Harbour Department and especially Clas Aspö for the seriousness and interest in the project. Furthermore, we appreciate the possibility of sitting at the company during the whole Thesis period and this way we gained an insight into how to combine the theoretical and practical fields. We would also like to thank Isak Björhag from Strusoft for help regarding the Pile feature in FEM-Design.

Finally, we want to thank our families for the moral support both during the years of studying and during the process of the Master's Thesis.

Gothenburg, June 2018

Michelle Skjærlund Fabrin and Osama Ali Bek

Notations

Roman upper letters:

A_{base}	Cross-section area of the pile base
B	Pile width
D	Cross-section diameter of the pile
E_p	Young's modulus of the pile
E_s	Young's modulus of the soil
E_{oed}	Constrained Young's modulus
E_{oed}^{ref}	Constrained Young's modulus at stress level p^{ref}
E_{ur}	Young's modulus at un-/reloading
E'_{ur}	Young's modulus at un-/reloading for effective stresses
E_{ur}^{ref}	Young's modulus at un-/reloading for stress level p^{ref}
EI	Pile rigidity
F_b	Internal force at the pile base
F_{si}	Internal force of one shaft segment, i
G_s	Shear modulus of the soil
$I_{p,z'}$	Moment of inertia of a cross-section of the pile
J_R	Non-dimensional term for L_u
K	Lateral earth pressure coefficient
K_0	Lateral earth pressure coefficient at rest
K_0^{NC}	Lateral earth pressure coefficient at rest for normal-consolidated soil
K_p	Passive earth pressure
$K_{x'}$	Shaft spring stiffness in x' -direction
$K_{x'_0}$	Base spring stiffness in x' -direction
$K_{y'}$	Shaft spring stiffness in y' -direction
$K_{z'}$	Shaft spring stiffness in z' -direction
L	Embedded pile length
L_c	Critical length of the embedded part of pile
L_{cr}	Critical buckling length
L_e	Equivalent pile length
$L_{element}$	Length of one division
L_s	Equivalent length of embedded part of pile
L_{tot}	Total length of the pile
L_u	Unembedded length
M	Compression modulus
M_0	Compression modulus at the over-consolidated stress levels
M_0	Compression modulus in the linear soil model
M_L	Compression modulus at the normal-consolidated stress levels
M_u	Compression modulus at insitu vertical effective stresses σ'_{v0}
M'	Rate of compression modulus at $\sigma'_L < \sigma'_v$
N_c	Bearing capacity coefficient

N_q	Bearing capacity factor
OCR	Over-consolidation ratio
P	Circumference of pile cross-section
P_{actual}	The actual external applied load
P_{cr}	Critical Euler load
R	Total resistance of the pile
R_b	Base resistance of the pile
R_R	Stiffness dependent parameter
R_s	Shaft resistance of the pile
S_R	Non-dimensional term for L_s

Roman lower letters:

c'	Drained shear strength of the soil for effective stresses
c_k	Drained characteristic shear strength of the soil
c_{uk}	Undrained characteristic shear strength of the soil
k_s	Constant soil stiffness in horizontal direction
l_{max}	Criteria for depending the embedded depth
m	Exponent for stress dependency in constitutive equations
m_{nc}	Normal-consolidated modulus number
m_{oc}	Over-consolidated modulus number
n	Number of buckling mode shapes
p^{ref}	Reference stress used in constitutive equations
p'_c	Mean effective pre-consolidation pressure at isotropic consolidation
p'_L	Mean effective limiting stresses at isotropic consolidation
p'_0	Mean effective stresses at isotropic consolidation
r_m	Radial distance of the pile
r_0	Pile radius
t	Material thickness

Greek upper letters:

$\Delta x'_b$	Displacement of the base segment in x'-direction
$\Delta x'_{si}$	Displacement of one pile segment, i , at the shaft in x'-direction

Greek lower letters:

α	Adhesion factor for undrained soil
α_{neg}	Factor for negative shaft friction for undrained soil
β	Friction coefficient multiplier for drained soil
β_{Euler}	Effective length factor
β_{neg}	Factor for negative shaft friction for drained soil
γ_s	Unit weight of the soil
γ_p	Unit weight of the pile
δ	Pile-skin friction angle
δ_H	Embedded ratio
κ^*	Modified swelling index
λ^*	Modified compression index
ν_p	Poisson's ratio of the pile

ν_s	Poisson's ratio of the soil
ν'_s	Elastic Poisson's ratio of the soil
ρ_m	Ratio between shear modulus
$\sigma'_1, \sigma'_2, \sigma'_3$	Effective principle stresses
σ'_c	Effective pre-consolidation pressure at 1D consolidation
σ'_L	Effective limiting stresses at 1D consolidation
σ'_v	Effective vertical stresses
$\sigma'_{v,a}$	Average effective vertical stresses
σ'_{v0}	Insitu effective vertical stresses
$\sigma'_{x0}, \sigma'_{y0}, \sigma'_{z0}$	Insitu effective stresses at rest
$\sigma'_x, \sigma'_y, \sigma'_z$	Effective stresses
ϕ'	Friction angle
ϕ_{cv}	Critical state friction angle
ϕ_k	Characteristic friction angle
ψ	Dilatancy angle

1

Introduction

1.1 Background

Port and marine structures connect ship traffic with road transport. The structures are located next to the water, which often results in challenging soil conditions since the sea has caused erosion and sedimentation in the past. For this reason shallow foundation for ports structures is often not possible and instead deep foundations have to be used. In this case, there is a risk of buckling of the pile since the pile is partially embedded in the water and partly in the soil. The load bearing part of a marine structure consists of a concrete slab supported by load-bearing piles, see Figure 1.1. Since the concrete foundation is categorised as a structural element and the load-bearing piles as geotechnical elements, design of port and marine structures needs to combine the two engineering fields, structural engineering and geotechnical engineering (Lai, 2012).



Figure 1.1: Example on a marine structure consisting of concrete slab supported by piles in water (Photo: © Concrete Consultants Group, 2017)

Finite Element Modelling (FEM) is used when the entire marine construction shall be analysed and designed. It requires the FEM software to combine geotechnical and structural engineering which is challenging and often an absence in many existing design tools. Today, the modelling of marine structures with deep foundations are

performed by dividing the analysis into two parts. The structural part is modelled directly in the FEM software while the load-bearing piles are defined as simple point supports on the concrete slab. These pile models consider only axial loading and stiffness and can only be hinged. The geotechnical pile analysis is performed afterwards in a separate software.

The software company Strusoft has in the previous years added geotechnical features to the mainly structural FEM software named FEM-Design 3D Structures. In version 17 of FEM-Design a new feature *Pile* is introduced which allows the user to model piles and connect them with other structures. It gives a possibility to model a complete marine structure in one FEM code instead of dividing and simplifying the design approach. The design process will become faster, more accurate and integrate the knowledge of geotechnical and structural engineering. The Port & Marine Department in the consultant company Ramböll is customer of Strusoft's FEM-Design and has for this reason an interest in this new Pile feature.

1.2 Aim of the Thesis

The aim is to validate geotechnical design and to verify structural design for the new Pile feature in the software FEM-Design 3D Structures version 17.

1.3 Objectives

The following questions will be answered in this Thesis:

Geotechnical Validation:

- How does FEM-Design model and analyse a pile?
- Does FEM-Design achieve reasonable results when compared to a field measurement test on an axial compressed bored pile with a solid cross-section:
 - Case 1 - Linear soil model.
 - Case 2 - Over-consolidated soil model.

Structural Verification:

- Does FEM-Design achieve reasonable results when an axial compressed driven pile with hollow cross-section is compared to analytical methods for buckling:
 - Case 3 - Partially embedded pile located in water and partly in soil.

1.4 Method

Literature studies, reading the software manuals and performing simple hand calculations have been used to understand the theory behind the Pile feature in FEM-

Design 3D Structures from the input to output data. The validation of the load-displacement behaviour has been achieved by comparing with Wehnert and Vermeer (2004) for the linear and the over-consolidated soil models. For the two cases the model parameters have been inset in FEM-Design and the output results have been compared with the pile load test. A sensitivity analysis has been performed in continuation of the two case studies. Furthermore, FEM-Design will also be used to verify buckling for partially embedded piles. The comparison in FEM-Design of the buckling analysis has been performed and compared with three analytical methods. The discussion and conclusion of the Thesis have been based on the results of the three comparisons and reflections on the cases where the software is applicable. Through these comparisons the Pile feature has been validated and verified.

1.5 Limitation of the Thesis

- Only load-displacement behaviour will be performed in geotechnical design while only buckling will be performed in structural design of the pile.
- Axial, single and end-bearing pile in compression with minimal installation effects will be chosen in the modelling.
- Negative skin friction in the modelling is ignored.
- The only FEM-software considered in the Thesis will be FEM-Design 3D Structures. Therefore, there is no comparison with other software programme.

1.6 Overview

The following is an overview of the Chapters in the Thesis:

- Chapter 2: *Modelling piles in FEM-Design*: Describes how soil and pile is modelled in FEM-Design including limitation of the software. The Chapter describes possible types of analyses and relevant output results.
- Chapter 3: *Validation of pile load test*: Compares the FEM-Design modelling with the pile load test. The results are compared and a sensitivity analysis is performed for relevant parameters.
- Chapter 4: *Verification of buckling load of partially embedded pile*: Compares estimation of equivalent pile length and critical buckling load from chosen analytical methods and FEM-Design.
- Chapter 5: *Conclusion*: Concludes the Thesis and give recommendations for using FEM-Design and further studies.

2

Modelling piles in FEM-Design

2.1 Modelling of the soil

The soil is modelled in FEM-Design as layers of strata where a ground water table is possible to include. Each stratum is selected as *drained* or *undrained* which affects the required input parameters. The required soil input values can be seen in Figure 2.1. The cohesion can be chosen as linearly depth increasing by use of d . The Reference Level moves the surface value of all depth depending parameters up or down. The software uses the input values for calculating the plastic limit forces, see Section 2.2.2. The soil model of FEM-Design can be selected as linear or, over-consolidated. A manually modifying over-consolidated soil model is called generic.

Foundation design
Deformation calculation
Both

Reference level [m] 0.000

Behaviour Undrained

Design according to combined behaviour

	Value	d
c uk [kN/m ²]		0.000
c k [kN/m ²]		0.000
phi k [deg]		
phi cvk [deg]		
Gamma dry [kN/m ³]		
Gamma sat. [kN/m ³]		

Figure 2.1: Required input values of the soil in FEM-Design.

2.1.1 Linear soil model

The input values of the linear soil model are based on Young's modulus E_s or compression modulus M_0 and Poisson's ratio ν_s . The linear soil model indicates the normal-consolidated compression modulus M_0 , while the over-consolidation soil model describes M_0 as the compression modulus at the over-consolidated stress levels. The soil model fits best with normal-consolidated and homogeneous soil without stress-history. Figure 2.2 shows the interface of the linear soil model in FEM-Design. E_s or the corresponding M_0 can be chosen as linear; constant or depth-dependent.

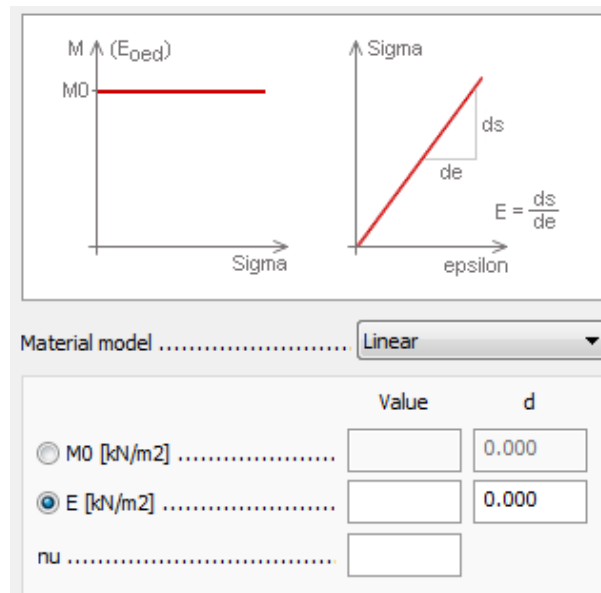


Figure 2.2: Interface of linear soil model in FEM-Design. FEM-Design determines Poisson's ratio ν_s as nu and E_s as E .

The linear soil model has an elastic behaviour with a linear relation between E_s , M_0 and ν_s . The following linear relations between the stiffnesses are used for all soil models in FEM-Design.

$$E_s = \frac{M_0(1 + \nu_s)(1 - 2\nu_s)}{1 - \nu_s} \quad (2.1)$$

$$G_s = \frac{E_s}{2(1 + \nu_s)} \quad (2.2)$$

2.1.2 Over-consolidated soil model

The input values of the over-consolidated soil model in FEM-Design can be obtained from e.g. a constant rate of strain test (CRS test), see Figure 2.3a. A CRS test is a oedometer test where the sample has been strained with a constant rate (Meijer and Åberg, 2007).

The over-consolidated soil model includes stress and depth-dependent stiffness and

stress-history. Figure 2.3b shows that the model is depending on the compression modulus on different effective stress levels (initial stress levels and during loading.)

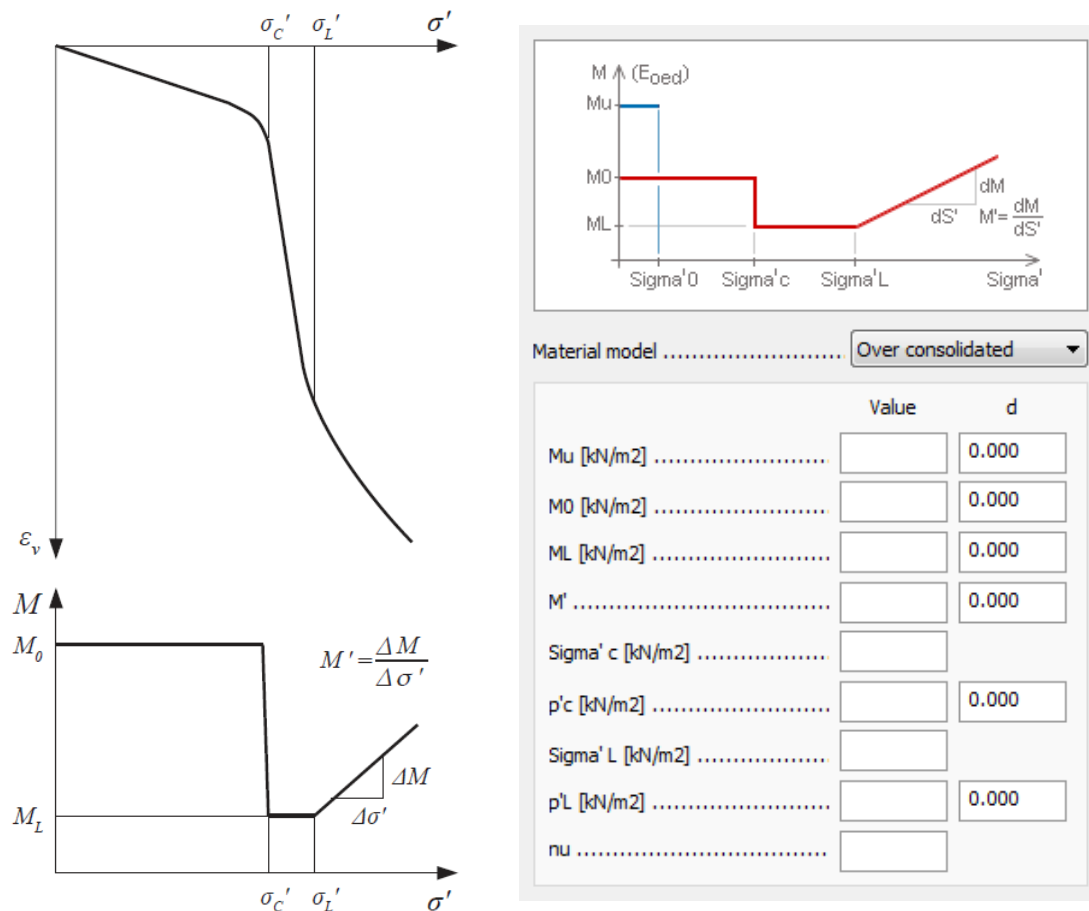


Figure 2.3: Figure 2.3a: Idealised CRS test and converting test data to software input in the over-consolidated soil model (Strusoft, 2016). Figure 2.3b: Interface of the over-consolidated soil model in FEM-Design. FEM-Design determines Poisson's ratio ν_s as nu .

The soil model, see Figure 2.3b, is based on three stress regions of one-dimensional consolidation; the over-consolidated region $0 < \sigma'_v < \sigma'_c$, the normal-consolidated region $\sigma'_c < \sigma'_v < \sigma'_L$ and beyond the normal-consolidated region $\sigma'_L < \sigma'_v$. The over-consolidated region is defined by the compression modulus M_0 and the effective pre-consolidated pressure σ'_c while the normal-consolidated region is defined by M_L and σ'_L . The stiffness beyond the normal-consolidated stress levels is obtained by the rate of compression modulus M' which is the difference of compression modulus depending on difference of vertical effective stress, see Figure 2.3b.

In general, the over-consolidated soil model in FEM-Design is a three-dimensional analysis. Though, when dealing with piles it is translated to a one-dimensional analysis. The software works with three-dimensional problem with isotropic consolidation; the isotropic mean effective pre-consolidation pressure p'_c and the isotropic mean effective limiting stresses p'_L . σ'_c and σ'_L consider one-dimensional consolidation. The relation between p' and σ' is unknown; though the relation is assumed

according to Equation (2.3) (Strusoft, 2016). p'_c , p'_L and the compression modulus can be chosen to increase linearly with the depth.

$$p'_0 = \frac{\sigma'_{x0} + \sigma'_{y0} + \sigma'_{z0}}{3} = \frac{K_0\sigma'_z + K_0\sigma'_z + \sigma'_z}{3} = \sigma'_z \left(\frac{2K_0 + 1}{3} \right) \quad (2.3)$$

$$\sigma'_{z'} = \sigma'_{x'} K_0 \quad (2.4)$$

The lateral earth pressure coefficient at the rest is assumed $K_0=0.5$ in Equation (2.3) and (2.4) as a default value in FEM-Design which gives p' to be 2/3 of vertical effective stresses. The relation between σ' and p' can be changed manually.

The generic soil model includes also implementation of stress history. It allows the user to choose an individual dependency of the relation between the compression modulus and the vertical effective stress after the mean effective pre-consolidation pressure p'_c .

2.2 Soil-pile interaction

2.2.1 Support stiffnesses

The interaction between the pile and the soil in FEM-Design is modelled according to Szakály (2017) provided by Strusoft. The interaction is represented by linear-elastic-perfectly plastic line supports at the shaft and one linear elastic-perfectly plastic point support at the pile top where each support has a stiffness and a plastic limit. Each support has a translational stiffness depending on the soil and pile properties. Each line support consists of three degrees of freedom: The horizontal stiffnesses $K_{y'}$ and $K_{z'}$ and the vertical stiffness $K_{x'}$ (Szakály, 2017). The point support at the pile tip consists of $K_{y'}$ and $K_{z'}$ and the vertical base stiffness $K_{x'_0}$. The intervals of the stiffnesses go from free restraint to rigid restraint. The stiffnesses in FEM-Design are shown on Figure 2.4. The resistances R_s and R_b are explained in Section 2.2.2.

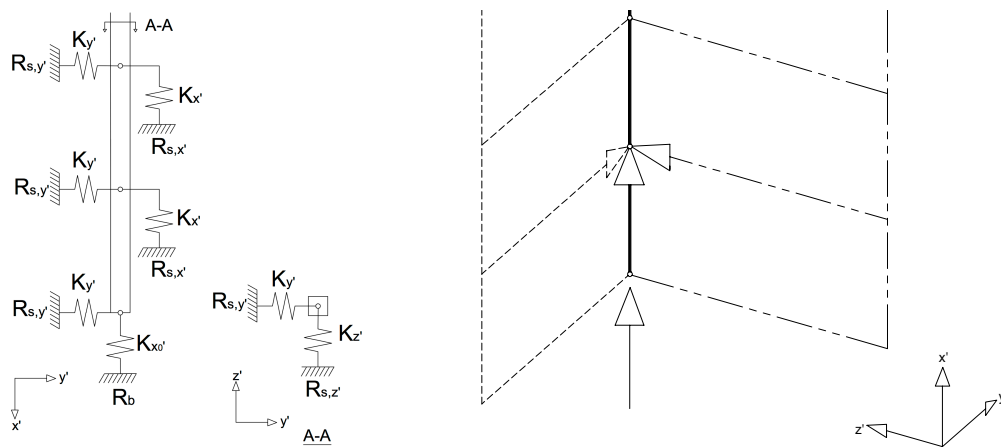


Figure 2.4: The stiffness principle used in the Pile feature at the shaft and base. $R_{s,y'}$ and $R_{s,z'}$ are not relevant in this Thesis since only non-eccentric axial loads are considered. Every shaft resistance mentioned in the report refers to $R_{s,x'}$.

Calculation of the horizontal stiffnesses, $K_{y'}$ and $K_{z'}$, is performed according to Vesic (1961):

$$K_{y'} = B \frac{0.65 E_s}{B(1 - \nu_s^2)} \left(\frac{E_s B^4}{E_p I_{p,z'}} \right)^{1/12} \quad [\text{kN/m}^2] \quad (2.5)$$

E_s and ν_s are Young's modulus and Poisson's ratio of the soil at each support. E_p and $I_{p,z'}$ are Young's modulus and moment of inertia of the cross-section of the pile. B is the pile width. Uniform soil stiffness is assumed in the y' and z' direction in this Thesis. For a non-eccentric loaded compression pile the output results are independent on the horizontal stiffnesses when buckling is disregarded.

The vertical shaft stiffness $K_{x'}$ affects the output results of a vertically loaded pile. The feature Piles in FEM-design builds on the principles of the Randolph and Wroth method (Knappett and Craig, 2012) for calculating $K_{x'}$ for an analytical solution according to Zhang et al. (2014):

$$K_{x'} = \frac{G_s}{r_0 \ln\left(\frac{r_m}{r_0}\right)} P \quad [\text{kN/m}^2] \quad (2.6)$$

In Equation (2.6) G_s is the shear modulus of the soil strata, P is the circumference of the pile cross-section, r_0 is the pile radius and r_m is the radial distance where the shear stresses of the soil are disregarded (Szakály, 2017):

$$r_m = 2.5 L \rho_m (1 - \nu_s) \quad (2.7)$$

$\rho_m = 1$ and L_{tot} is the total length of the pile in soil for a pile with one homogeneous soil layer without depth increasing properties.

The vertical stiffness at the pile tip, $K_{x'_0}$, is calculated according to Zhang et al. (2014):

$$K_{x'_0} = \frac{4G_s r_0}{(1 - \nu_s)} \quad [\text{kN/m}] \quad (2.8)$$

The software calculates the stiffnesses automatically according to the input values; though the stiffnesses can be modified manually.

2.2.2 Plastic limit forces

FEM-Design specifies the axial total resistance of the pile as plastic limit force R which is the sum of the axial shaft resistance R_s and axial base resistance R_b depending on the drainage condition and the input parameters (Szakály, 2017). The resistances are calculated according to the α or β -methods which are described in the following. When the utilisation of each support in the shaft and base has reached 100 %, failure occurs in the pile.

The α -method is used for undrained cohesive soil with total stresses. The calculation

of the resistances includes the characteristic undrained shear strength c_{uk} . The vertical shaft resistance in FEM-Design is calculated as Szakály (2017):

$$R_s = \alpha c_{uk} P \quad [\text{kN/m}] \quad (2.9)$$

α is the adhesion coefficient depending on the pile material and the cohesion soil according to NAVFAC (1986), see Table 2.1. The software chooses the average value of α in the specific interval. Normally, α is recommended to be $0.7 < \alpha < 1.0$ for normal-consolidated and slightly over-consolidated soil and down to $\alpha = 0.4$ for over-consolidated soil (Alén, 2012). It fits well into the values of Table 2.1 since over-consolidated soil has higher cohesion.

Table 2.1: The determination of α in FEM-Design (NAVFAC, 1986).

Pile type	Soil consistency	Undrained shear strength c_u [kPa]	α
Timber and concrete piles	Very soft	0 - 12	1.00
	Soft	12 - 24	1.00 - 0.96
	Medium stiff	24 - 48	0.96 - 0.75
	Stiff	48 - 96	0.75 - 0.48
	Very stiff	96 - 192	0.48 - 0.33
Steel piles	Very soft	0 - 12	1.00
	Soft	12 - 24	1.00 - 0.92
	Medium stiff	24 - 48	0.92 - 0.70
	Stiff	48 - 96	0.70 - 0.36
	Very stiff	96 - 192	0.36 - 0.19

The base resistance in FEM-Design is determined the following way:

$$R_b = A_{base} c_{uk} N_c \quad [\text{kN}] \quad (2.10)$$

The bearing capacity coefficient is in FEM-Design always chosen as $N_c = 9$ (Skempton, 1959) which is a conservative value.

The β -method considers the drained case with effective stresses. The shaft resistance in FEM-Design is determined as:

$$R_s = \beta \sigma'_{v,a} P \quad [\text{kN/m}] \quad (2.11)$$

$\sigma'_{v,a}$ is the average of the effective vertical stresses at the certain depth. β depends on the pile-skin friction angle δ and the lateral earth pressure coefficient K , see Equation (2.12). FEM-Design chooses K as the average value in Figure 2.3 depending on the installation method of the pile and the direction of the force. The software does not distinguish between the lateral earth pressure coefficient for diameters larger or smaller than 60 cm for bored piles; it will always be chosen $K=0.7$. Though, the

values of K and δ can be modified manually.

$$\beta = \tan(\delta)K \quad (2.12)$$

Table 2.2: The determination of the pile-skin friction angle δ in FEM-Design according to NAVFAC (1986).

Pile type	Pile-soil interface friction angle (δ)
Steel piles	20°
Timber piles	$3/4\phi'$
Concrete piles	$3/4\phi'$

Table 2.3: The determination of the lateral earth pressure coefficient K for piles in compression and tension in FEM-Design according to NAVFAC (1986).

Pile type	K (compression)	K (tension)
Driven H-piles	0.5 - 1.0	0.3 - 0.5
Driven displacement piles (round & square)	1.0 - 1.5	0.6 - 1.0
Driven displacement tapered piles	1.5 - 2.0	1.0 - 1.3
Driven jetted piles	0.4 - 0.9	0.3 - 0.6
Bored piles (less than 60 cm in diameter)	0.7	0.4

The base resistance R_b in drained soil is determined:

$$R_b = A_{base}(\sigma'_{v,a}N_q + c_k N_c) \quad [\text{kN}] \quad (2.13)$$

The bearing capacity factors N_q and N_c depend on the installation method and friction angle shown in Table 2.4. The software chooses the boundary value for N_q when the actual friction angle is outside the interval of Table 2.4.

$$N_c = (N_q - 1) \cot(\phi_k) \quad (2.14)$$

Table 2.4: Determination of N_q according to NAVFAC (1986).

ϕ' [°]	26	28	30	31	32	33	34	35	36	37	38	39	40
N_q for driven piles	10	15	21	24	29	35	42	50	62	77	86	120	145
N_q for bored piles	5	8	10	12	14	17	21	25	30	38	43	60	72

2.3 Modelling of the pile

The Pile feature of FEM-Design models the pile as a one-dimensional bar with line supports along the shaft and one point support at the tip. The material of the pile model in compression has a linear response.

The compressible pile is divided into a series of divisions separated by linear elastic-perfectly plastic supports representing the soil-pile interaction, see Figure 2.5. The accuracy of the interaction can be chosen by the length of the division $L_{element}$; the smaller the length of the division the more detailed the output results will be. The length of the division can be chosen between 0.1 m and 100 m.

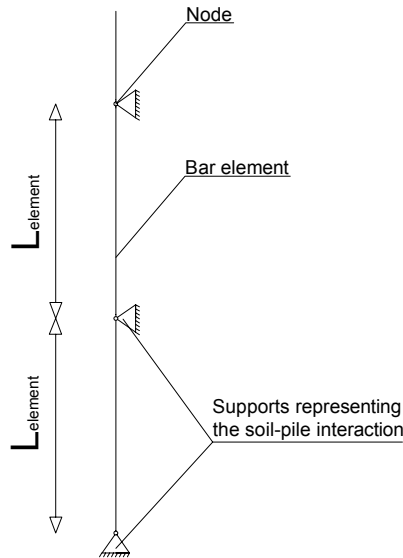


Figure 2.5: Principles of divisions, nodes and supports of FEM-Design.

Regular and composite materials in different dimensions are available to model the cross-section of the pile. The pile head can be modelled as free, hinged or fixed to describe the connection to the structural element above. This end connection can also be modified manually in terms of stiffnesses. The installation method can be chosen as bored, driven displacement or driven jetted pile, which will influence the total resistance according to Table 2.3.

The modelling of the pile has the ability to consider the effect of negative shaft friction, also called drag-down. The software generates the effect automatically above the neutral plane, if the value of α_{neg} or β_{neg} has been inset. FEM-Design includes ordinary load, structural dead load and negative shaft friction by consideration of the duration class according to EN 1995-1-1. The relevant load combinations for pile modelling are the ultimate and characteristic limit state.

2.4 Analyses

The Pile feature in FEM-Design has the ability to run different types of analyses.

- Linear elastic analysis
- Non-linear elastic analysis
- Non-linear plastic analysis

Section 2.4.1-2.4.3 describes the behaviour of the three analyses. This Thesis follows the geotechnical sign convention where compression is determined as positive and tension as negative.

2.4.1 Linear elastic analysis

The linear elastic analysis is characterised by linear elastic behaviour of the shaft and base without considering failure. The shaft and the base have identical behaviour for tension and compression, see Figure 2.6. All the shaft and base of the supports will increase linearly when a load is applied resulting in linear-elastic behaviour of both resistances. The base modelling is a simplification of the real behaviour, since the base resistance of pile in tension is zero in reality.

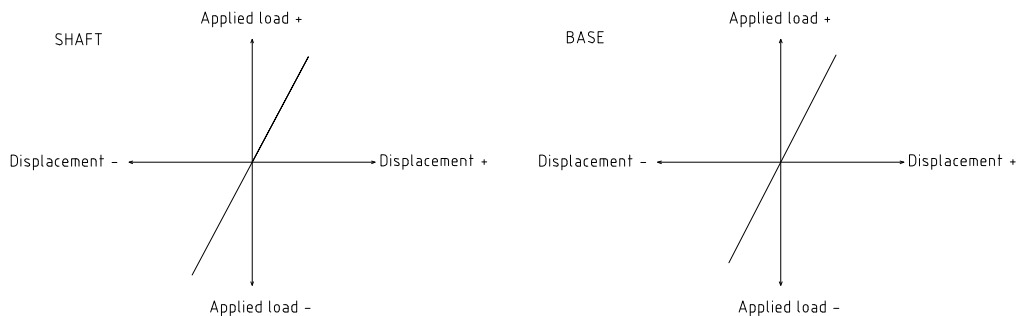


Figure 2.6: Compression-tension behaviour for a linear elastic analysis with shaft (left) and base (right) separated.

2.4.2 Non-linear elastic analysis

In the non-linear elastic analysis the base and shaft behaviours are also linear. However, the base resistance is zero when the pile is subjected to axial tension load which is only the difference between the linear and non-linear analysis, see Figure 2.7. The shaft has the same behaviour in case of axial compression and tension loads.

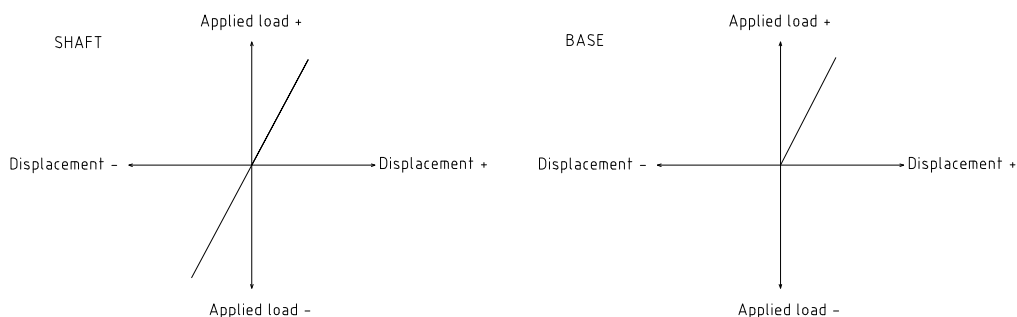


Figure 2.7: Compression-tension behaviour for a non-linear elastic analysis with shaft (left) and base (right) separated.

2.4.3 Non-linear plastic analysis

In the non-linear plastic analysis the plastic limit is considered for both shaft and base resistance, see Section 2.2.2. Above the plastic limit failure will occur which FEM-Design describes as *large nodal displacement or rotation was found*, see Figure 2.8. It means that failure in the soil-pile interaction has been occurred resulting in very large displacement. The shaft and base have different behaviours in the plastic analysis since the shaft has non-linear behaviour while the base has linear behaviour until reaching the failure load, see Figure 2.8.

The soil-pile interaction is represented by point and line supports where each support has a linear elastic-perfectly plastic behaviour. All supports at the shaft behave with a non-linear behaviour. However, the plastic limit has a strong effect on the behaviour of these supports. The line supports are distributed along the pile shaft divided by a number of divisions where each support has defined a plastic limit. The limit is increasing with the depth. When a small load is applied the shaft supports closest to the external load will reach their plastic limits first but never go above since failure then happens. The rest of the supports has at this point not reached their plastic limits. If the load is increased further makes more supports will reach their plastic limit. This distribution results in a non-linear behaviour of the shaft. The base consists of only one support and the base resistance has a linear relation between the applied load and the displacement of the base resistance until the reaching its plastic limit, see Figure 2.8. The base will be fully utilised after the shaft.

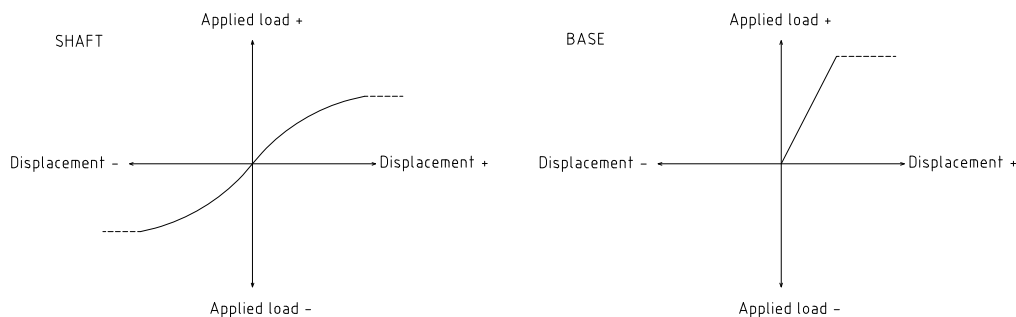


Figure 2.8: Compression-tension behaviour for a non-linear plastic analysis with shaft (left) and base (right) separated.

2.5 Output results

2.5.1 Translational displacement

FEM-Design calculates the translational displacement along the shaft at each node for a pile in compression. By summarising the translational displacements for all division the total compression of the pile can be found. The displacement depends on the stiffnesses of the shaft and base and for the non-linear plastic analysis also the plastic limit. The displacement at the top of an axial-loaded pile in compression describes the instantaneous displacement of the pile - also called pile head

displacement. Here it is assumed that the soil is displaced in one dimension. Elastic analyses do not include any plastic limits while the plastic analysis gives a very high translational displacement when reaching the plastic limit.

2.5.2 Reactions

The software has the ability to show the development of reaction forces at each support at the shaft and the base. The distribution of the reactions looks different depending on the chosen analysis.

The linear and non-linear elastic analyses show a simultaneous linear increase of all support reactions at the shaft and base since the plastic limits of the supports are not included in the two calculations. Therefore, the reaction forces will increase continuously since failure in the supports is not possible, see Figure 2.9a.

In the plastic analysis, the plastic limit is considered which means that the support reactions cannot go above their plastic limit. When the load is applied, the closest support reactions get fully utilised first. When the load is further increasing, more supports reach their plastic limits, see Figure 2.9b-2.9d.

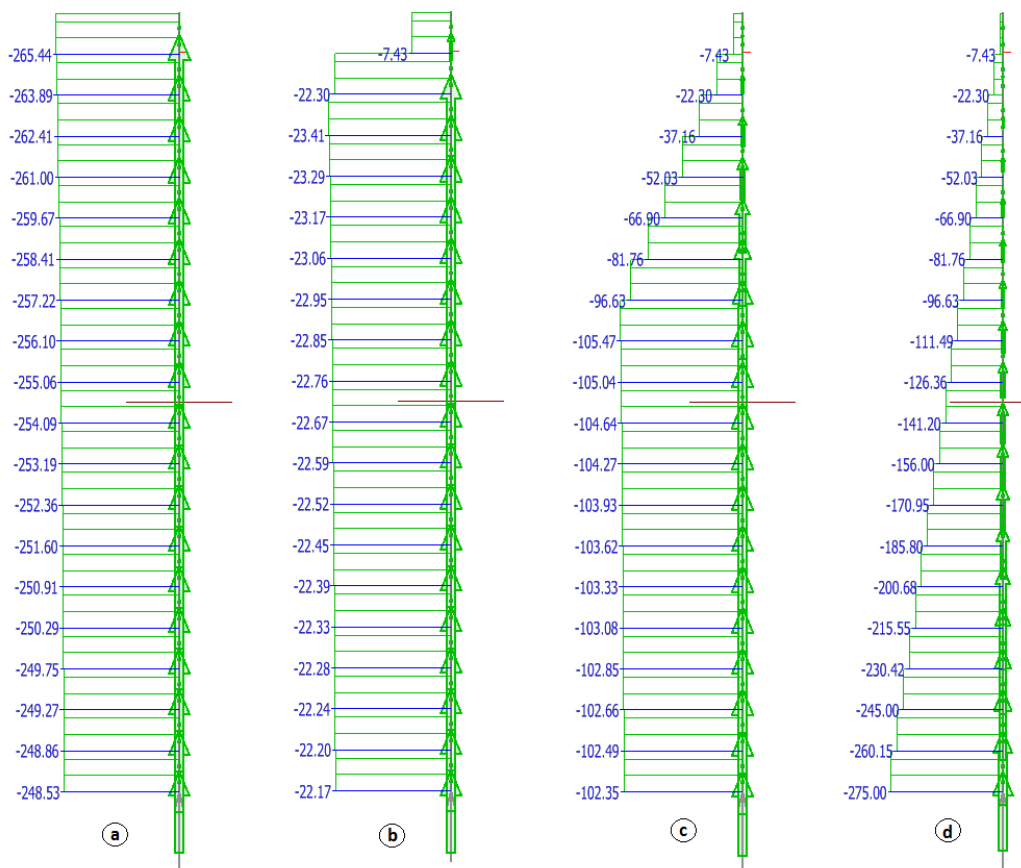


Figure 2.9: Development of reaction forces for the three types of analysis. Figure 2.9a: A static axial compression load in the linear and non-linear elastic analyses. Figure 2.9b-2.9d: An increasing axial compression load in the plastic analysis.

The ultimate load is when all the support reactions at the shaft and the base reach their plastic limit, see Figure 2.9d. Above the ultimate load, failure occurs in support reactions representing the soil-pile interaction. Failure in FEM-Design realises very large translational displacement, see also Section 2.5.1.

2.5.3 Internal forces

The pile model is divided into a series of divisions, where the software calculates the internal forces as well as the internal stresses depending on the cross-section at each node. The internal forces depend on the pile head displacements and the soil stiffness in addition to the applied load. It results in a linear or non-linear distribution depending on the type of analysis. The distribution of the internal forces along the pile is linear in the elastic analysis. The internal force F_{si} of an arbitrary shaft segment, i , depends on the vertical displacement of the pile segment $\Delta x'_{si}$ and the vertical shaft stiffness $K_{x'}$ (Knappett and Craig, 2012):

$$F_{si} = F_{si+1} + K_{x'} \left(\frac{\Delta x'_{si} + \Delta x'_{si+1}}{2} \right) \quad (2.15)$$

The internal force at the base F_b in FEM-Design is depending on the vertical base stiffness $K_{x'_0}$ and the vertical displacement of the base segment $\Delta x'_b$.

$$F_b = K_{x'_0} \Delta x'_b \quad (2.16)$$

While in the plastic analysis, the internal force distribution is non-linear. However, the maximum values of the internal force have been obtained when both the shaft and base have reached their plastic limits.

2.6 Limitation of FEM-Design

The Pile feature is a simplification of the real pile behaviour. FEM-Design models the soil as linear elastic-perfectly plastic supports along the pile instead of three dimensional solid soil elements. Due to these simplifications the software has the following limitations which may influence the output results.

- The pile is modelled as a one dimensional linear elastic bar without failure.
- The soil-pile interaction is represented by supports on the pile. The pile head displacement is assumed to be one dimensional for axial load. Therefore, only one dimensional problems can be considered in the modelling. The soil failure cannot be simulated since the failure line are not shown in the calculation.
- In the non-linear plastic analysis, the linear elastic relationship between the applied load and pile head displacement can be obtained until reaching the plastic limit. When the load is increased further the plastic limit, failure will happen and the displacement goes to infinity.

2. Modelling piles in FEM-Design

- Long term effects of the pile material like creep and shrinkage are includable in the software but the output results consider only instantaneous calculation.
- Long term effects in soil are not included in the analyses since FEM-Design always assumes that the excess water pressure has been dissipated. Therefore, all analyses are performed in the final state, since time is not a variable in FEM-Design.
- The software works only for internal force and displacement and not for the design capacity calculations.
- The generation of the shaft and base supports is independent on the soil width and length as long as the whole pile is covered.

FEM-Design does in certain cases illogical assumptions, which are not described in Strusoft (2016) or Szakály (2017). These are mentioned in Appendix A.

Table 3.1 shows the relevant input parameters from the pile load test obtained by El-Mossallamy in Wehnert and Vermeer (2004) which has been used in the following FEM-Design modelling. In Table 3.1, the soil parameters fit the normal consolidated clay.

Table 3.1: Selected pile and soil parameters for Case 1 (Wehnert and Vermeer, 2004).

Pile input	Value	Unit	Soil input	Value	Unit
γ_p	25	kN/m ³	γ_s	20	kN/m ³
E_p	30000	MN/m ²	c'	20	kN/m ²
ν_p	0.2	-	ϕ'	20	°
Material	Concrete	C20/25	ψ	0	°
			E_s	60	MN/m ²
			ν_s	0.3	-
			K_0^{NC}	0.8	-

In Wehnert and Vermeer (2004) there are performed three FE-analyses based on Sommer & Hammbach and El-Mossallamy. The pile behaviour in the FE-analyses was assumed to be linear elastic and the subsoil behaviour was described by the elastic-plastic Mohr-Coulomb model (MC), the Soft Soil model (SS) (based on modified Cam-Clay model) and the Hardening Soil model (HS).

3.3 Modelling the pile in FEM-Design

A bored pile with large diameter of 1.3 m and length of 9.5 m has been modelled in FEM-Design v17. The soil has a depth of 20 m and a width of 25 m and consists of homogenous, tertiary stiff, over-consolidated clay. Drained condition is chosen in the modelling including a ground water table at -3.5 m. The pile is modelled as a one-dimensional bar element, the pile model behaviour is linear-elastic and the pile material is plain concrete C20/25.

The line and point supports are generated representing the soil-pile interaction at the base and shaft as linear elastic-perfectly plastic supports with stiffness in the x', y' and z' directions, see Figure 3.2. The division length is set to 0.5 m resulting in 19 divisions along the pile shaft.

The pile model is subjected to a non-eccentric axial compression force. Hence, the horizontal displacements are assumed to be zero. The non-linear plastic analysis is used for the calculations of the pile model. The loading is simulated by increase of the load starting from zero until reaching the plastic limit. For each load step the pile head displacement is measured and plotted into a figure.

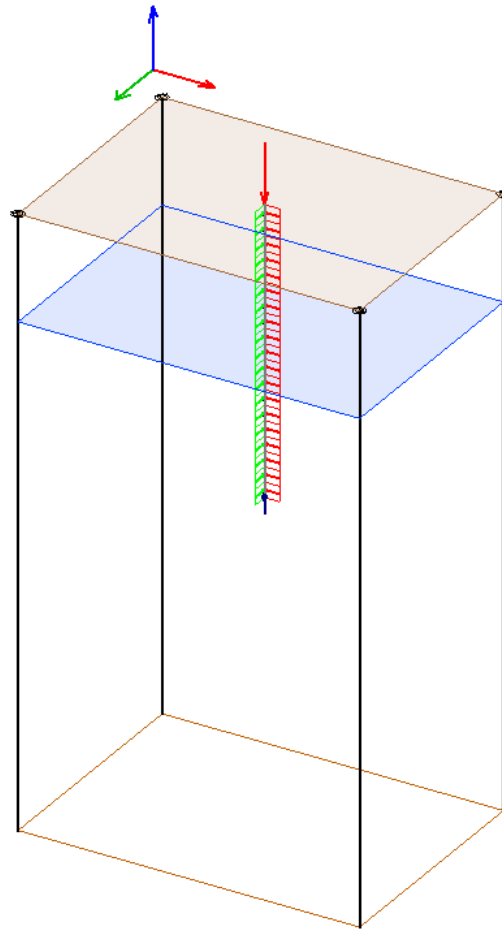


Figure 3.2: Modelling of the fully embedded pile including ground water level at -3.5 m.

3.4 Case 1 - Linear soil model

3.4.1 Introduction

The linear soil model is selected in Case 1 which depends on the soil properties E_s and ν_s from Table 3.1 which are constant and not stress or depth-dependent. When the excavation of the pile shaft is performed, only a very small change of in-situ effective stresses will occur which makes the assumption reasonable $K \approx K_0^{NC}$ (Fleming et al., 2009). Based on this reason the installation effect of the bored pile can be ignored in the Thesis.

Since the analysis is performed in drained fine-grained soil it is assumed that the pile skin friction angle δ' has a perfectly rough interface (Knappett and Craig, 2012). Therefore $\delta' = \phi'$ can be chosen.

3.4.2 Results & discussions

The following shows and discusses the performance of the software and the results of the pile model and pile load test for Case 1. The results are divided into the diagrams

3. Validation of pile load test

showing the applied load versus pile head displacement of the total resistance and the separated shaft and base resistances of the pile. This to clarify the behaviour of each resistance.

The ultimate load of the pile model has been reached when the plastic limit forces of the shaft and base are fully mobilized. Therefore, the total resistance of the pile is the sum of ultimate resistances of the shaft and the base. The behaviour of the pile load test may include plastic deformation, non-homogeneous soil layers, a complicated drainage conditions and a not fully rough friction interface which FEM-Design does not consider. The software simplifies the drainage condition since it always assumes that the excess water pressure has been dissipated. Therefore, the analysis is performed in the final state which means the time is not a variable in FEM-Design. In reality, the stiff clay will not be 100% drained but only be drained to certain extents for each layer.

For the total resistance the lateral earth pressure capacity K has been regulated for Case 1. The input data of Table 3.1 assumes normal-consolidated soil. However, the lateral earth pressure coefficient has been increased to $K=1$ to consider the over-consolidation effect.

Figure 3.3 shows the applied load versus head pile displacement for the total resistance in case of the pile load test and the two pile model cases of FEM-design when $K=0.8$ and 1.0 .

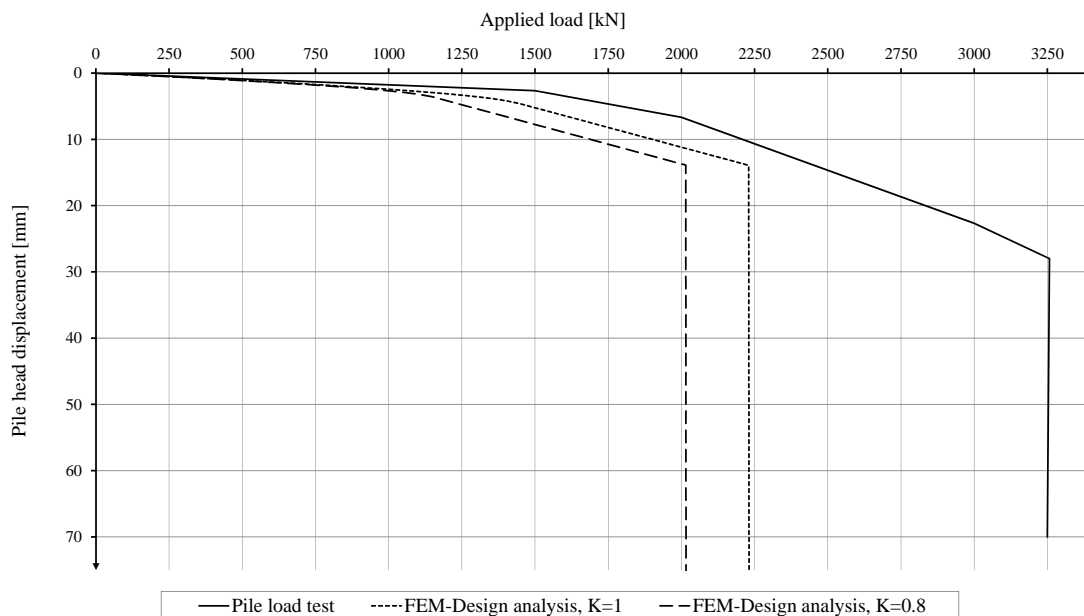


Figure 3.3: Case 1: Total resistance for analysis in FEM-Design in case of $K=0.8$ ($R=2015$ kN) and $K=1$ ($R=2230$ kN) and pile load test (Wehnert and Vermeer, 2004).

As Figure 3.3 shows the increased value to $K=1$ gives a higher ultimate load and a stiffer behaviour of the total resistance. It is reasonable according to Equation (2.11)

and (2.12). An increasing of K does not reach the ultimate load of the pile load test. Though the increased K gives resistance and stiffness closer to the pile load test. However, the lateral earth pressure coefficient depends on the soil properties, installation method and stress history according to Knappett and Craig (2012) and can be difficult to determine accurately.

A more detailed behaviour of the pile is examined by separating the shaft and the base as the following shows where $K=1$.

In Figure 3.4, the applied load has been plotted versus the pile head displacement for the pile model in Case 1 and the pile load test when only the base is activated. In FEM-Design the behaviour has been modelled by setting the support stiffness of the shaft to be *free*.

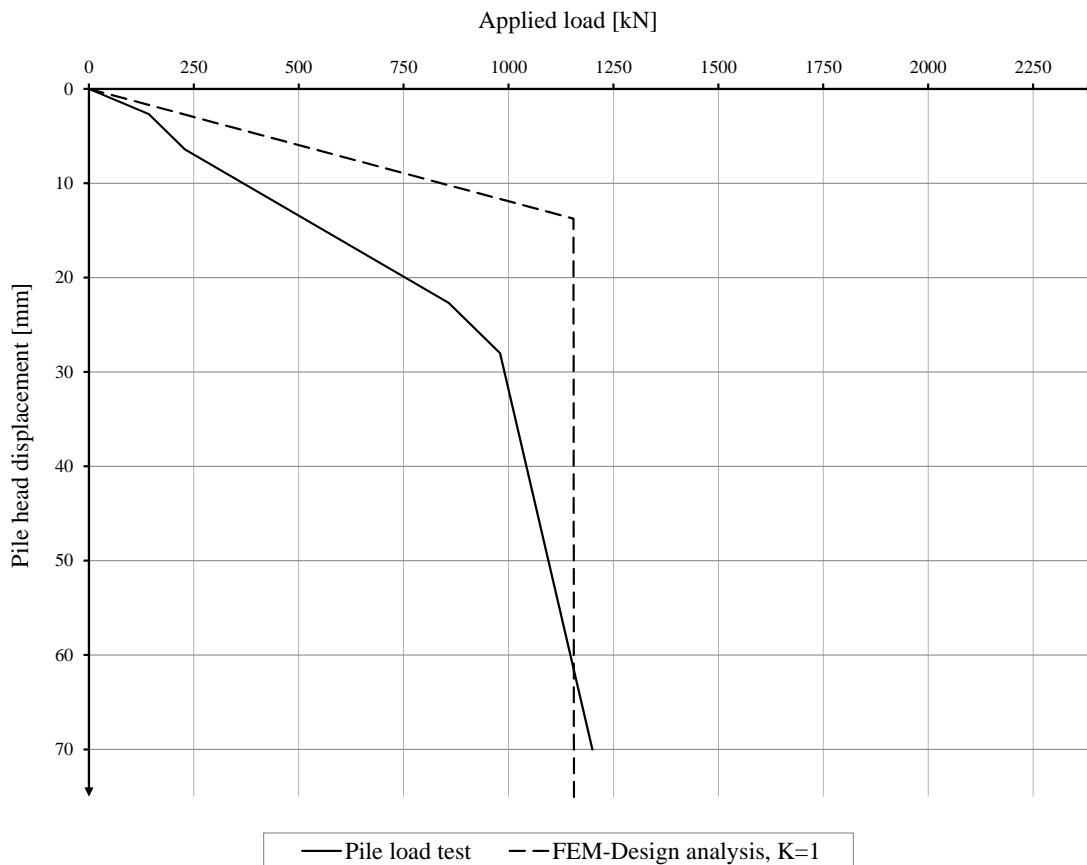


Figure 3.4: Case 1: Base resistance for analysis in FEM-Design with $K=1$ ($R_b=1155$ kN) and pile load test (Wehnert and Vermeer, 2004).

The pile model shows a stiffer behaviour than the pile load test though the ultimate loads are almost identical. The relationship between the applied load and the pile head displacement is described by a bi-linear relationship. It does not describe the real behaviour of the non-linear base resistance since the pile-soil interaction at the base is modelled with one linear elastic-perfectly plastic support. Furthermore, the

3. Validation of pile load test

pile model shows an infinity pile head displacement when reaching the plastic limit, see Figure 3.4.

To clarify the shaft behaviour Figure 3.5 shows the comparison between the shaft resistance of the pile load test and the analysis of the pile model performed for Case 1. The two results are plotted as pile head displacement versus applied load.

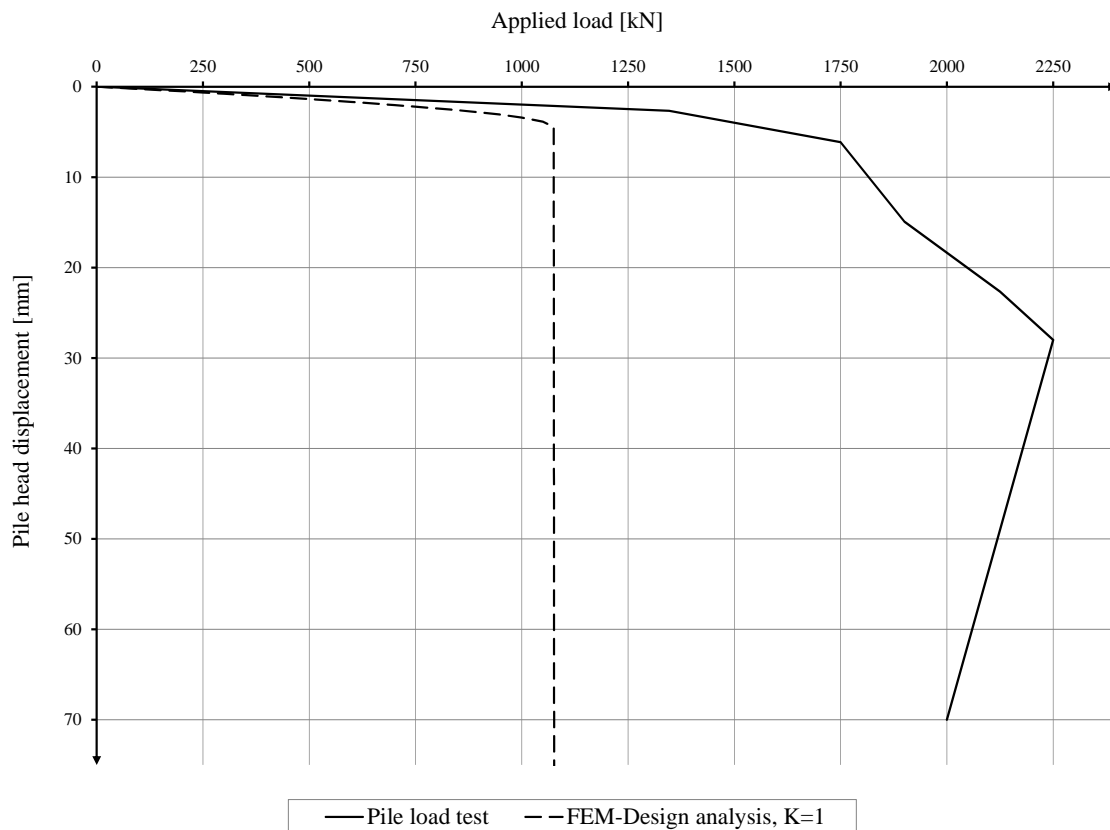


Figure 3.5: Case 1: Shaft resistance for analysis in FEM-Design with $K=1$ ($R_s=1075$ kN) and pile load test (Wehnert and Vermeer, 2004).

At very small loads the pile model and the pile load test have similar behaviour, see Figure 3.5. When the load is increased, the pile load test shows a stiffer behaviour since the input values of the pile model has normal-consolidated properties. There is a big difference of ultimate load between the pile load test and the pile model. The ultimate load of the shaft resistance has been reached when all the divisions along the pile have achieved their plastic limit. Plastic deformation is not includable for the pile model in FEM-Design; though the ultimate load could increase more this way.

3.5 Case 2 - Over-consolidated soil model

3.5.1 Introduction

The results in Case 1 show that the linear soil model gives simplified stiffness behaviour since the chosen stiffness E_s is constant. The soil model is changed to the over-consolidated soil model for Case 2 by use of the Hardening Soil parameters from Table 3.1 since they can be converted to the over-consolidated soil model. The over-consolidated soil model includes a more advanced stiffness behaviour and is expressed by three stress-dependent compression modulus M , see Figure 2.3.

The soil input data of Wehnert and Vermeer (2004) does not include a CRS test which can be used to find parameters to the over-consolidated soil model. For this reason the input data shown in Figure 2.3 are assumptions together with the choice of the lateral earth pressure coefficient K . Three different methods are developed to estimate the compression modulus at different stress levels, M_0 and M_L , based on the available soil properties in Wehnert and Vermeer (2004). Afterwards, the results of the pile head displacement of the total, shaft and base resistances are plotted and compared with the pile load test.

3.5.2 Input values

The following assumptions compensate for the absence of over-consolidated soil properties in Wehnert and Vermeer (2004). Originally, the input values of the over-consolidated soil model can be obtained from the CRS test as mentioned in Section 2.1.2.

For Case 2 the lateral earth pressure coefficient $K_0 \approx K$ will be calculated to fit the ultimate load of the tested pile. $K \approx K_p = 2$ has been found by use of Equation (3.1) for passive earth pressure. It leads to $\beta = 0.73$ according to Equation (2.12). According to Parry and Swain (1977) the β value for bored piles in drained conditions is $0.5 < \beta < 1.5$.

$$K_p = \frac{1 + \sin \phi'}{1 - \sin \phi'} \quad (3.1)$$

By use of Equation (3.2) the over-consolidation ratio will be $OCR=9.24$ (Knappett and Craig, 2012).

$$K_0 = (1 - \sin(\phi'))\sqrt{OCR} \quad (3.2)$$

The pre-consolidation pressure σ'_c can be found as a function of the vertical effective pressure σ'_v and therefore depth increasing (Knappett and Craig, 2012).

$$OCR = \frac{\sigma'_c}{\sigma'_v} \quad (3.3)$$

The following relation between effective limiting stress σ'_L and the pre-consolidated

pressure σ'_c is assumed.

$$\sigma'_L \approx 10\sigma'_c \quad (3.4)$$

The mean effective pre-consolidation stresses p'_c and p'_L can be found according to Equation (2.3) depending on lateral earth pressure coefficient at the rest.

The over-consolidated soil model used in Case 2 has been simplified to only include the compression modulus of the over-consolidated part M_0 and the normal-consolidated part M_L . For this reason the rate of compression modulus at $\sigma'_L < \sigma'_v$ has been chosen $M' = 0$. Furthermore, it is assumed that the compression modulus at insitu vertical effective stresses $M_u = M_0$ since installation effects of the bored pile have been ignored.

Three different methods have been used to estimate M_0 and M_L . A common characteristic of all methods is that they are FE-relations which considers stress formulations in three dimensions while FEM-Design does only work in one-dimension. Therefore, the three methods are assumptions. The available input values from Wehnert and Vermeer (2004) are used in Method 1-3 to find the parameters in the over-consolidated soil model.

- Method 1: M_0 and M_L are found by empirical FE-relations for a Soft Soil Creep (SSC) model by considering the modified swelling κ^* and compression λ^* index. The method is relevant for $\lambda^*/\kappa^* = 5 - 10$ while in Wehnert and Vermeer (2004) $\lambda^*/\kappa^* = 3$ which leads to that Method 1 is insufficient to use (Olsson, 2010).
- Method 2: The case builds on combinations of Karlsrud and Janbu empirical relations found in *Creep in soft soil* by Frankisek Havel (Havel, 2004) and *Back Calculation of Measured Settlements for an Instrumented Fill on Soft Clay* by Stian Berre (Berre, 2017). The over-consolidated modulus number m_{oc} and normal-consolidated modulus number m_{nc} are calculated from κ^* and λ^* and inserted in the Janbu relations at each stress level. M_0 will be constant while M_L will depend on the vertical effective stresses σ'_v . Method 2 assumes a constant compression modulus M_0 which is not stress-dependent and does not consider stress history. Therefore the method is insufficient to use.
- Method 3: The case builds on FE-relations from Hardening Soil model (Karstunen and Amavasai, 2017). Furthermore it includes linear relations between E'_{ur} and M_0 (Karstunen and Amavasai, 2017) and assumes $E'_{oed} = M_L$ and uses Equation (2.1) and (2.4).

Method 3 will be used in the over-consolidated soil model. A detailed description of finding M_0 and M_L is found below and the existing input values from Wehnert and Vermeer (2004) are shown in Table 3.2.

Young's modulus for unloading and reloading at effective stresses E'_{ur} depends on

Young's unloading/reloading modulus at the reference stress level p^{ref} , E_{ur}^{ref} , see Equation (3.5). The exponent m depends on the stress dependency and equals $m = 0.5$ for over-consolidated soil models like Hardening Soil Model (Wehnert, 2006).

$$E'_{ur} = E_{ur}^{ref} \left(\frac{c' \cos(\phi') + \sigma'_3 \sin(\phi')}{c' \cos(\phi') + p^{ref} \sin(\phi')} \right)^m \quad (3.5)$$

All parameters in Equation (3.5) are found from Wehnert and Vermeer (2004) expect the horizontal effective principle stresses $\sigma'_3 = \sigma'_h$ which will be calculated from the effective vertical stresses according to Equation (2.4). Here it is estimated that $K_0 \approx K$. Furthermore, ν'_s is the elastic Poisson's ratio which is estimated $\nu'_s \approx \nu_s = 0.3$.

$$M_0 = \frac{(1 - \nu'_s) E'_{ur}}{(1 - 2\nu'_s)(1 + \nu'_s)} \quad (3.6)$$

The normal-consolidated compression modulus M_L is estimated from the formulation of the Hardening Soil Model and is similar to Equation (3.5). Equation (3.7) shows according to Wehnert (2006) that the constrained Young's modulus E_{oed} is equal to the normal-consolidated compression modulus M_L (Karstunen and Amava-sai, 2017).

$$M_L = E_{oed} = E_{oed}^{ref} \left(\frac{c' \cos(\phi') + \sigma'_1 \sin(\phi')}{c' \cos(\phi') + p^{ref} \sin(\phi')} \right)^m \quad (3.7)$$

Equation (3.7) is depth and stress-dependent due to the vertical effective principle stresses $\sigma'_1 = \sigma'_v$.

Table 3.2: Soil properties from Wehnert and Vermeer (2004) for finding M_0 and M_L at Case 3.

FEM input parameters	Value	Unit
E_{oed}^{ref}	33	MN/m ²
E_{ur}^{ref}	90	MN/m ²
p^{ref}	100	kN/m ²
m	0.5	-

Table 3.3 and Table 3.4 show the chosen input values for the over-consolidated soil model. The rest of the soil input parameters is shown in Table 3.1. The pile-soil interaction friction angle is chosen identical to Case 1. The soil layers have been divided into *dry* and *saturated* parts since the compression modulus M and the mean effective stresses p' are depending on the effective stresses which are different above and below the ground water table.

3. Validation of pile load test

Table 3.3: Estimated dry input parameters for the over-consolidated soil model at level 0 to -3.5 m for $K=2$ (Wehnert and Vermeer, 2004). d is the increase of the certain value for 1 meter, see also Figure 2.1.

Dry soil input	Value	Unit	d	Unit
M_u	74.121	MN/m ²	10089	m
M_0	74.121	MN/m ²	10089	m
M_L	20.189	MN/m ²	2748	m
M'	0	-	0	m
σ'_c	0	kN/m ²	-	-
p'_c	0	kN/m ²	308	m
σ'_L	0	kN/m ²	-	-
p'_L	0	kN/m ²	3080	m
ν_s	0.3	-	-	-

Table 3.4: Estimated saturated input parameters for the over-consolidated soil model at level -3.5 m to -9.5 m for $K=2$ (Wehnert and Vermeer, 2004). d is the increase of the certain value for 1 meter, see also Figure 2.1.

Saturated soil input	Value	Unit	d	Unit
M_u	95.693	MN/m ²	3889	m
M_0	95.693	MN/m ²	3889	m
M_L	26.065	MN/m ²	1059	m
M'	0	-	0	m
σ'_c	539	kN/m ²	-	-
p'_c	539	kN/m ²	154	m
σ'_L	5390	kN/m ²	-	-
p'_L	5390	kN/m ²	1540	m
ν_s	0.3	-	-	-

3.5.3 Results & Discussions

Figure 3.6-3.8 show the comparison between the pile load test and pile model separated into total, shaft and base resistance. The modification of stiffness in Case 2 does not effect the plastic limit of the pile model but the lateral earth pressure coefficient does. The K has been fitted the ultimate load of the pile load test to make the behaviour of the pile model and pile load test close to each other. A comparison between the over-consolidated and the linear soil model has also been performed in order to understand the difference between the two models.

The ultimate load of pile model is the plastic limit, though the ultimate load of the pile load test is more complicated to find. Fellenius (2018) shows and discusses different methods for finding the ultimate load. Though, it requires that the behaviour of the pile model fits approximately the pile load test. This is not the circumstances for Case 1 and 2.

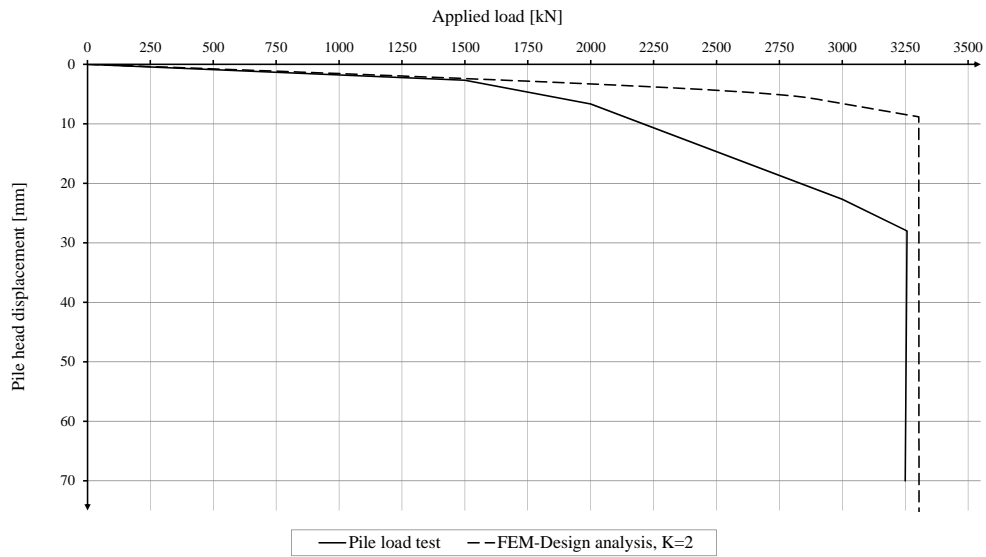


Figure 3.6: Case 2: Total resistance for analysis in FEM-Design with $K=2$ ($R=3304$ kN) and pile load test (Wehnert and Vermeer, 2004).

Even by increasing the lateral earth pressure coefficient to $K=2$ and use of the over-consolidated soil model the behaviour does still not match the pile load test. The pile model behaves stiffer than the pile load test, though they have nearly identical behaviour for load below 1500 kN. Furthermore, the pile model does not seem to include stress-dependent stiffness. In general, the pile model of Case 2 has a stiffer behaviour than Case 1, see Figure 3.3 and Figure 3.6. The shaft and base have been separated and plotted as applied load versus pile head displacement in Figure 3.7 and Figure 3.8 where they are compared with the pile load test.

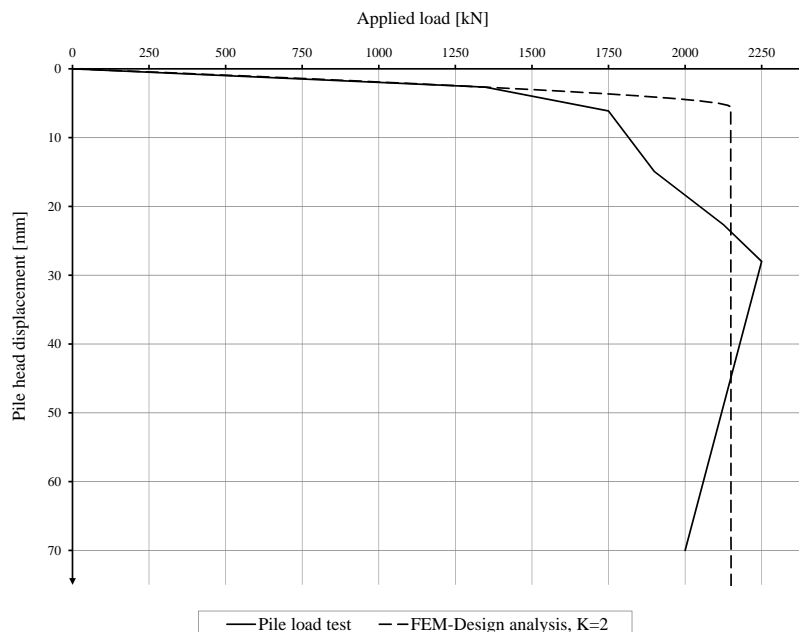


Figure 3.7: Case 2: Shaft resistance for analysis in FEM-Design with $K=2$ ($R_s=2149$ kN) and pile load test (Wehnert and Vermeer, 2004).

3. Validation of pile load test

The pile model and pile load test of the shaft have similar stiffness below 1400 kN. Though, the pile model has a stiffer and more simplified behaviour for loads above 1400 kN compared to the pile load test. In general, the pile model does not match the real behaviour by the use of the over-consolidated soil model, but it still has a better result compared to Case 1. The behaviour of the pile model in Case 2 shows a stiff behaviour than Case 1, see Figure 3.5.

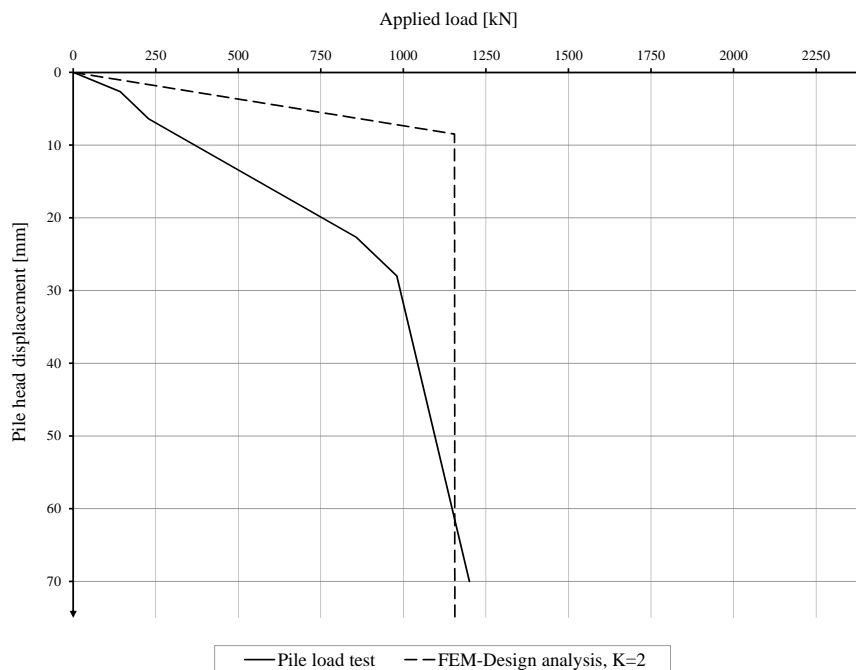


Figure 3.8: Case 2: Base resistance for analysis in FEM-Design with $K=2$ ($R_b=1155$ kN) and pile load test (Wehnert and Vermeer, 2004).

The ultimate loads of the base in Case 1 and 2 are identical, though Case 2 has a stiffer behaviour, see Figure 3.4 and 3.8. The reason is that the base consists of one single support which has a linear elastic-perfectly plastic behaviour where Case 1 has a higher stiffness. Furthermore, the same ultimate loads of the pile base in Case 1 and Case 2 are obtained according to Equation (2.13).

Figure 3.9 shows a comparison between the over-consolidated and linear soil model in order to analyse the difference in stiffness behaviour for the two soil models. Furthermore, Figure 3.9 shows also a comparison between FEM-Design analyses and an analysis performed with the Mohr Coulomb soil model obtained from Wehnert and Vermeer (2004). M_0 for the over-consolidated soil model is assumed according to Table 3.1 and Equation (2.1) and $K=1$ is used according to Case 1. The rest of input values of the over-consolidated soil model is identical to Table 3.4 and 3.3.

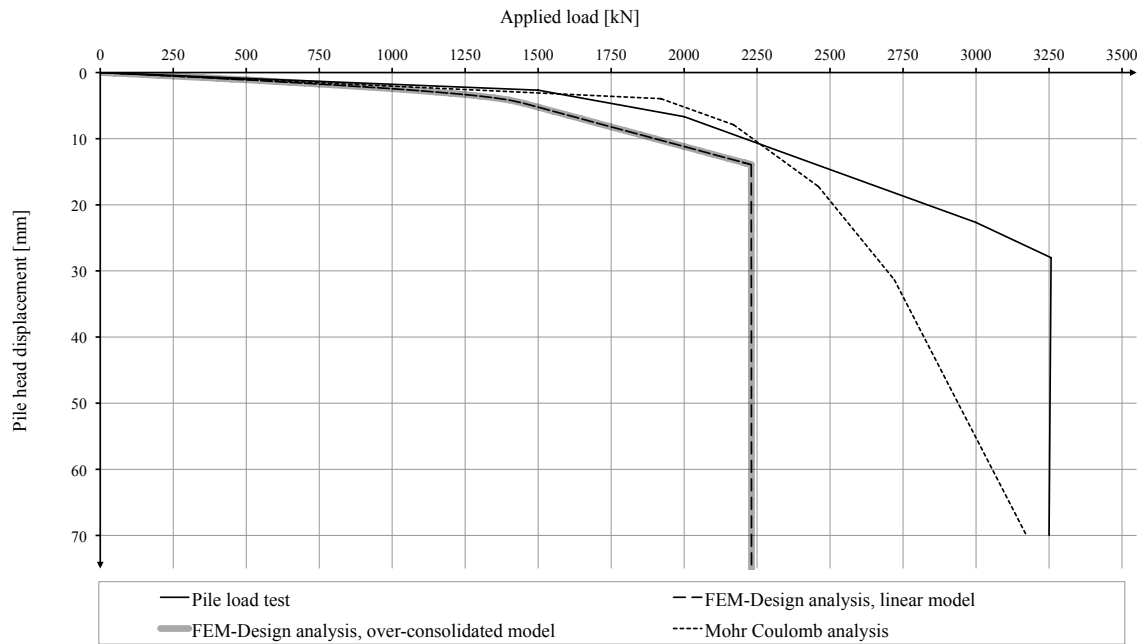


Figure 3.9: Case 2: Total resistance for analysis in FEM-Design with linear soil model, over-consolidated soil model and pile load test and analysis performed with Mohr Coulomb soil (Wehnert and Vermeer, 2004).

Figure 3.9 shows that the over-consolidated soil model has exactly identical behaviour as the linear model in the case when the same M_0 and K are used for the both models. It means that the over-consolidated model always considers M_0 (even for the normal-consolidated region) for generating the support stiffnesses and the over-consolidated soil model is not stress-dependent during loading. The generation of the stiffnesses is still linearly increasing.

The over-consolidation pressure σ'_c has been found according to Equation (3.3) which influences that M_0 always will be used for Case 2 since $\sigma'_v < \sigma'_c$. For cases with higher σ'_v other compression modulus should be used.

The comparison between the analyses of FEM-Design and the analysis with Mohr Coulomb soil model shows that the behaviour differs for applied loads above 1000 kN. The ultimate load of the Mohr Coulomb soil model is closer to the pile load test and seems to include plastic deformation. The Mohr Coulomb mode has constant stiffness and should behave less stiffer than the load pile test which Figure 3.9 shows.

3.6 Sensitivity analysis

Relevant input parameters from Wehnert and Vermeer (2004) are used to do a sensitivity analysis of FEM-Design including the linear soil model. The sensitivity analysis has been performed by stepwise increasing and decreasing the specific input value. The plastic limit and the pile head displacement just before failure have been found for each increment or decrement. The output results are compared with a

3. Validation of pile load test

standard case to evaluate the sensitivity.

FEM-Design determines the total resistance and pile head displacement by use of design equations and not FE-formulas which makes the sensitivity analysis to some extent simplified. Table 3.5 shows the tested input parameters and an estimation of how sensitive the parameters are.

Table 3.5: Results of the sensitivity analysis performed on relevant input values of Wehnert and Vermeer (2004) with the linear soil model.

Tested parameter	Very sensitive	Sensitive	Not sensitive
Young's modulus of soil		X	
Young's modulus of pile			X
Lateral earth pressure coefficient		X	
Pile length		X	
Friction angle of clay	X		
Cross-section diameter of pile		X	

The only *very sensitive* tested parameter is the friction angle where especially the large angles should be chosen very carefully. The relation between friction angle and total resistance (and pile head displacements) is acting exponentially in the interval 26-40°, see also Table 2.4 and Equation (2.14). The *sensitive* parameters show a clear linear relation between increase of tested parameter and increase of resistance and/or pile head displacement. The *not sensitive* parameters show only a small or no increase of total resistance and pile head displacements.

4

Verification of buckling load of partially embedded pile

4.1 Introduction

Buckling instability is a critical problem in structural design of slender piles since the failure will suddenly occur and may lead to collapse of the structure. In general, pile buckling is relevant in structural design for the following cases:

- During the driving of the piles.
- Fully embedded piles in soft clay and very loose sand.
- Partially embedded piles with a part in soil and a part in water or air.

As this Thesis focuses on marine structures, buckling instability of the partially embedded piles is often a problem and will be analysed in this Chapter. The verification is done for Case 3 based on the analytical methods due to lack of the experimental tests and due to not enough information of the existed experimental tests. The analytical methods are established by:

- Davisson and Robinson (1965)
- Heelis et al. (2004)
- Fleming et al. (1992)

Each of them have predicted the critical buckling load and equivalent length of the embedded part of the partially embedded pile.

The verification is carried out by a comparison between the critical buckling load and equivalent length of the embedded part of the pile model and the results estimated by analytical methods. The pile is subjected to axial compression load. The soil around the embedded part of the pile has a constant stiffness k_s while the unembedded part is in air.

4.2 Estimation of critical buckling load and equivalent length

4.2.1 Analytical methods

Three analytical methods has been analysed and the solution has found for the partially embedded pile with free unembedded end condition, see Figure 4.1a. The solutions are based on estimation the equivalent length of embedded part of the pile L_s , which is the length to the fixity, to convert the partially embedded pile to unembedded pile, see Figure 4.1b. Hence, the critical buckling load P_{cr} is defined for equivalent pile that corresponding to the equivalent unembedded length $L_e = L_u + L_s$ based on the Euler's Equation.

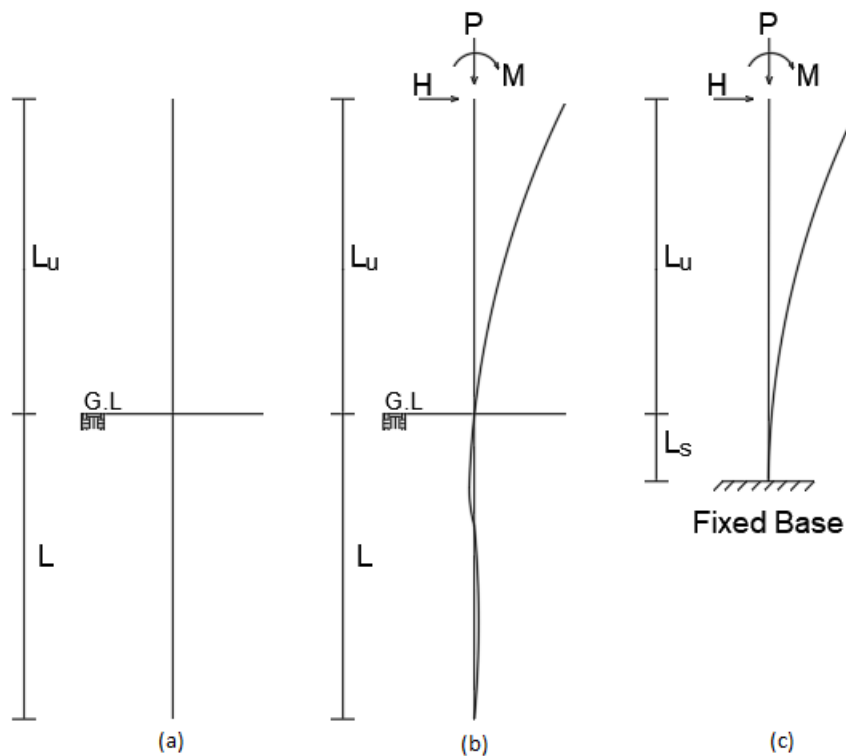


Figure 4.1: Partially embedded pile according to Davisson and Robinson (1965). a) Actual pile. b) Deformed shape under applying load. c) Equivalent pile.

The first solution, Davisson and Robinson (1965), is based on the non-dimensional terms such as J_R , S_R and I_{max} for estimation the equivalent length L_s and the critical buckling load P_{cr} for the equivalent pile, see Figure 4.2.

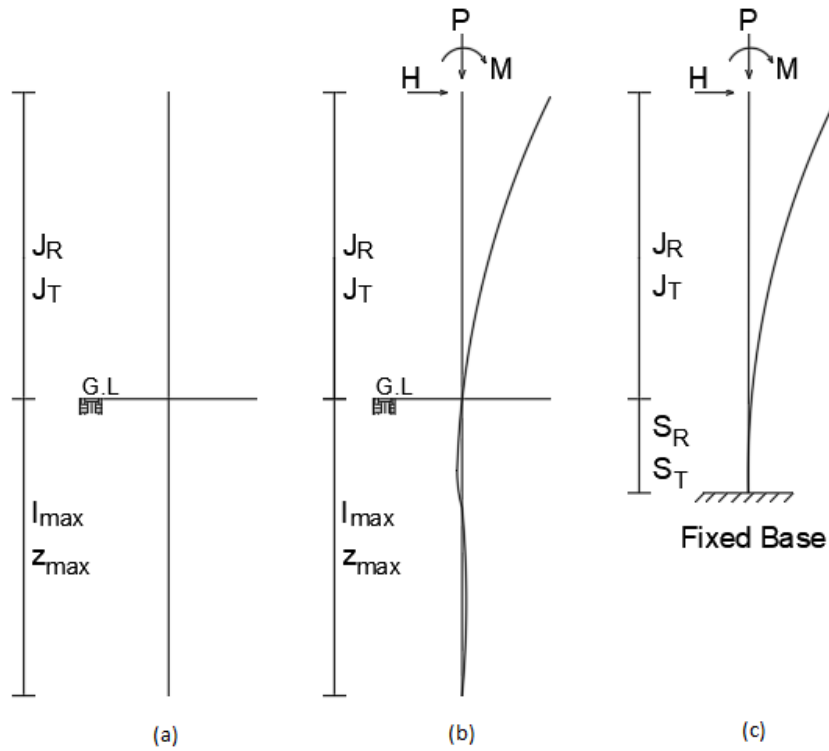


Figure 4.2: Partially embedded pile shown with non-dimensional terms according to Davisson and Robinson (1965). a) Actual pile. b) Deformed shape under applying load. c) Equivalent pile.

The non-dimensional terms J_R , S_R and l_{max} are assigned for constant soil stiffness and they can be found according to following equations:

$$J_R = \frac{L_u}{R_R} \quad S_R = \frac{L_s}{R_R} \quad l_{max} = \frac{L}{R_R} \quad (4.1)$$

where:

$$R_R = \sqrt[4]{\frac{EI}{k_s}} \quad (4.2)$$

EI is the pile rigidity while $k_s = \text{constant}$, is the soil stiffness in the horizontal direction. R_R has the unit length depends on the soil and the pile stiffness. J_R and S_R are the non-dimensional terms of the unembedded length L_u and the equivalent length L_s of the equivalent pile L_s , respectively. The relationship between J_R and S_R that are adopted by Davisson and Robinson (1965) displays in Figure 4.3a depending on the pile end conditions. The use of the Figure 4.3a requires the criteria of $l_{max} > 4$; then the embedded depth of the piles is large enough to be considered infinity long.

The second solution, Heelis et al. (2004), is also based on the non-dimensional terms. It uses the same equations as presented in Davisson and Robinson (1965). However, Heelis et al. (2004) has been presented the relation between S_R and J_R depending on the pile end condition and the embedded ratio $\delta_H = (L_u + L)/L$.

4. Verification of buckling load of partially embedded pile

Figure 4.3b and Figure 4.3c show the cases for free-free pile and fixed-translating-free pile, respectively.

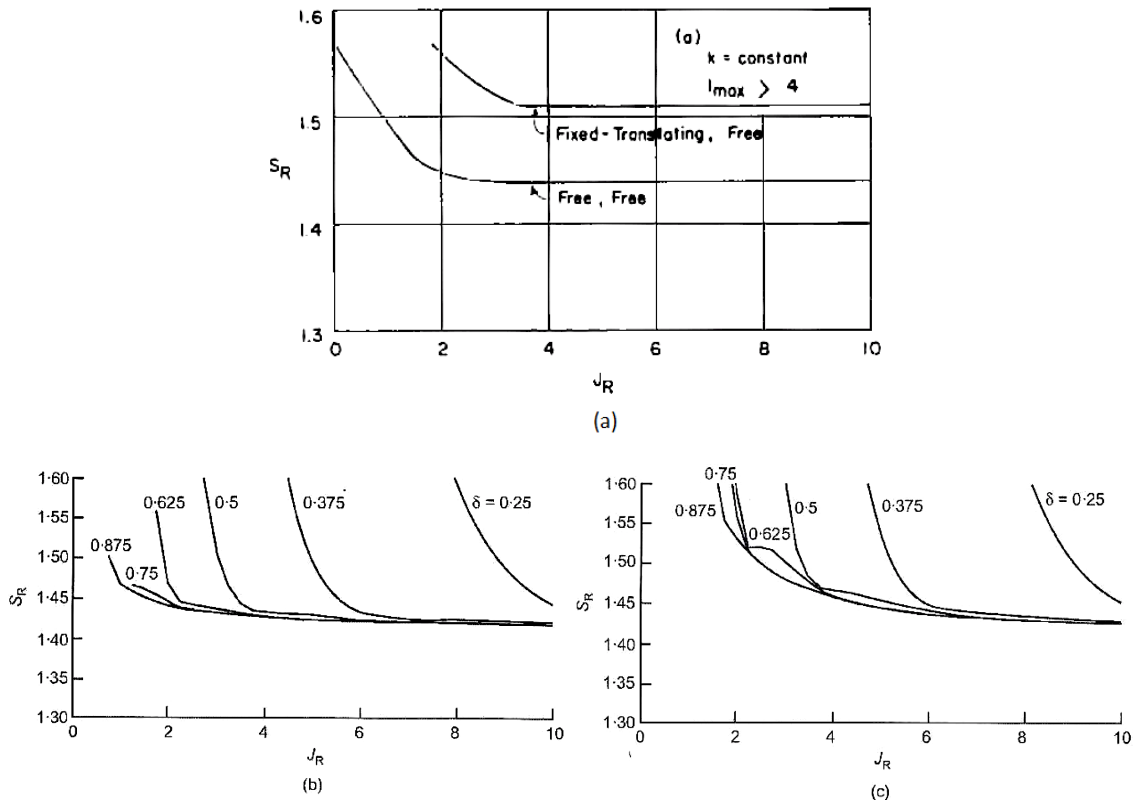


Figure 4.3: Equivalent length of the embedded part of the pile in non-dimensional terms with constant soil stiffness k_s and axial load: Calculated by Davisson and Robinson (1965) (top), calculated by Heelis et al. (2004) for free-free pile (left), calculated by Heelis et al. (2004) for fixed-translating pile (right).

Hence, the critical buckling load P_{cr} can be determined for the equivalent pile with free-fixed end conditions shown in Figure 4.1b under axial compression load.

$$P_{cr} = \frac{\pi^2 EI}{4(S_R + J_R)^2 R_R^2} \quad (4.3)$$

EI is the pile rigidity.

The third solution, Fleming et al. (1992), is similar to Davisson and Robinson (1965) in case of a partially embedded pile. The critical buckling load of the partially embedded pile can be found in Equation (4.4).

$$P_{cr} = \frac{\pi^2 EI}{4(L_u + L_s)^2} \quad (4.4)$$

L_u is the unembedded length and L_s is the equivalent length of the embedded part of the pile (length to fixity) which is found by:

$$L_s \approx 2 \left(\frac{EI}{k_s} \right)^{(1/4)} \quad (4.5)$$

Fleming et al. (1992) presents the critical length L_c . If the embedded length $L >$ the critical length L_c the pile behaves as it was infinity long; no increase in critical buckling load will be obtained after this critical length.

$$L_c = 2L_s \quad (4.6)$$

Equation (4.4) according to Fleming et al. (1992) is similar to the definition in Equation (4.3) according to Davisson and Robinson (1965). Both of them are based on Euler Equations for calculating the critical buckling load of the equivalent pile for free-fixed end conditions. Heelis et al. (2004) suggests for Equation (4.4) to replace the factor 4 with 0.25 for fixed end conditions, from 4 to 0.49 for pinned end condition and for translation-no-rotation unembedded end conditions from 4 to 1.

4.2.2 FEM-Design

In the stability analysis of FEM-Design, the Critical Parameter can be found which is the critical buckling load P_{cr} over the actual applied load P_{actual} , see Equation (4.7). If Critical Parameter < 1 , the structural element is unstable. if it is > 1 it is not.

$$\text{Critical parameter} = \frac{P_{cr}}{P_{actual}} \quad (4.7)$$

In addition, deformed shape can be obtained from the calculation of the stability analysis, see Figure 4.4. The critical buckling length L_{cr} can be found by interpreting the deformed shape.

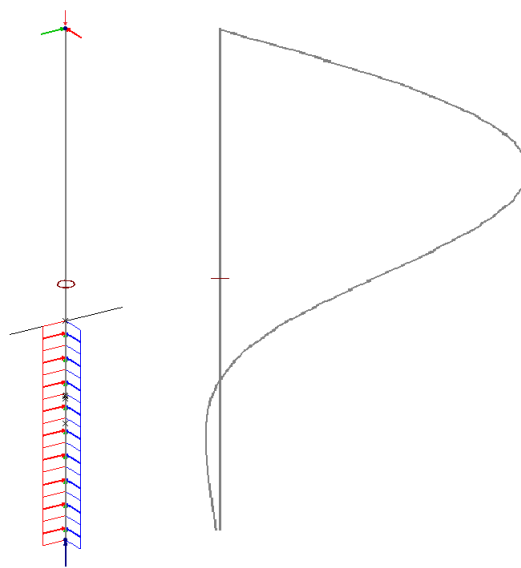


Figure 4.4: Partially embedded pile in FEM-Design. The actual pile (left) and the deformed shape (right).

Stability analysis in FEM-Design can be performed on bar elements. The analysis is based on Euler's critical load considering the number of buckling mode shapes n , the pile rigidity EI and support conditions at the critical buckling length L_{cr} , see Equation (4.8). $n=1$ gives the most critical case.

$$P_{cr} = \frac{(n\pi)^2 EI}{L_{cr}^2} \quad (4.8)$$

In this section the pile is partially embedded in which part of it is surrounded by the soil. However, the soil has a horizontal stiffness K_y and K_z according to Equation (2.5) which leads to resist the pile buckling. The critical buckling load P_{cr} is depending on the critical pile length L_{cr} . As Equation (4.9) shows L_{cr} is the sum of the unembedded L_u and the equivalent embedded pile length L_s .

$$L_{cr} = \beta_{Euler} L_{tot} = \beta_{Euler} (L_u + L_s) \quad (4.9)$$

β_{Euler} is the effective length factor.

4.3 Case 3 - Partially embedded pile

A partially embedded pile is in Case 3 chosen as a hollow-cylindrical steel pile driven into soil with diameter $D = 323.9$ mm, material thickness $t = 16$ mm, Young's modulus $E_p = 210$ GPa and unembedded length $L_u = 10$ m. The unembedded part is surrounded by air since the effect of the water is disregarded, while the embedded part is surrounded by stiff clay with constant stiffness where the Young's modulus $E_s = 60000$ kN/m² resulting with a constant stiffness $K_{y'} = K_{z'} = 30533$ kN/m² according Equation (2.5).

The unembedded end condition of the pile is chosen as fixed-translation with no rotation while the embedded end condition has a degree of freedom based on the soil-pile stiffness in three directions. The linear soil model is chosen.

Several embedded lengths L are tested in FEM-Design in order to predict the critical length L_c . For prediction of the equivalent length L_s and the critical buckling load P_{cr} , the embedded length is set as $L_s = L_c$ and several unembedded lengths L_u are chosen at this stage.

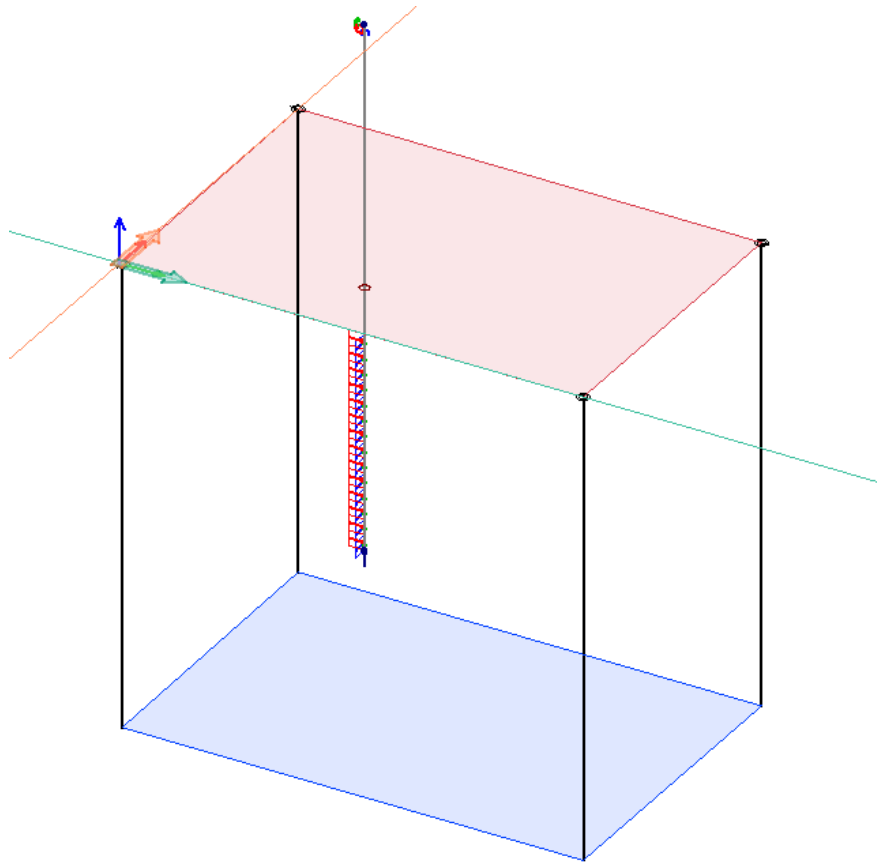


Figure 4.5: Partially embedded pile model in FEM-Design

4.4 Results & Discussions

The results below consist of the comparison of critical lengths of embedded pile part L_c and the comparison of equivalent lengths of the embedded pile part L_s and the critical buckling load.

The critical buckling load P_{cr} , which is a function of the embedded lengths L , is shown from FEM-Design in Table 4.1. L_u is constant. It is clear to notice that the maximum critical buckling load is achieved at $L=4.5$ m. This length can be considered as the critical length L_c since P_{cr} is almost constant beyond 4.5 m.

Table 4.1: Critical buckling load P_{cr} with constant unembedded length $L_u=10$ m for different embedded lengths L from FEM-Design.

L [m]	1	2	3	3.5	4	4.5	5	6	8	10
P_{cr} [kN]	1262	2394	2804	2847	2857	2859	2858	2858	2857	2859

The critical length $L_c=4.5$ m corresponding to the maximum buckling load in FEM-Design is compared with the analytical methods, see Table 4.2. It is clear to notice that Davisson and Robinson (1965) and Fleming et al. (1992) have identical critical

4. Verification of buckling load of partially embedded pile

length. However, in FEM-Design the critical length is close to what predicated according to analytical methods.

Table 4.2: Comparison of the critical lengths L_c for different analytical methods and FEM-Design.

Method	L_c [m]
FEM-Design analysis	4.5
Davisson and Robinson (1965)	4.24
Fleming et al. (1992)	4.24

The results of the prediction of the critical buckling load P_{cr} is shown in Table 4.3 for FEM-Design, Davisson and Robinson (1965), Fleming et al. (1992) and Heelis et al. (2004). The pile has been modelled for the embedded length $L=L_c=4.5$ since the critical buckling load after L_c is more or less constant and the unembedded lengths $L_u=3, 6$ and 10 m.

Table 4.3: Comparison of the critical buckling load P_{cr} [kN] for different unembedded lengths.

Method	$L_u=3$ m	$L_u=6$ m	$L_u=10$ m
FEM-Design analysis	18185	6671	2859
Davisson and Robinson (1965)	17920	6597	2832
Fleming et al. (1992)	14534	5779	2594
Heelis et al. (2004)	18511	6718	2863

The comparison shows that the FEM-Design results are close to the analytical methods results; Davisson and Robinson (1965) and Heelis et al. (2004). However, the critical buckling load that is predicted by Fleming et al. (1992) is underestimated.

Table 4.4 presents the equivalent length L_s of the embedded part of the pile according to the three analytical methods for different unembedded lengths L_u . It should be noticed that the equivalent length is almost constant at these lengths. It can be concluded that the equivalent length does not influence the change of unembedded length.

Table 4.4: Comparison of the equivalent length L_s [m] for different unembedded lengths.

Method	$L_u=3$ m	$L_u=6$ m	$L_u=10$ m
Davisson and Robinson (1965)	1.612	1.601	1.601
Fleming et al. (1992)	2.121	2.121	2.121
Heelis et al. (2004)	1.538	1.532	1.530

Since the prediction of the critical buckling load according to the analytical methods matched the results of FEM-Design approximately, the results of the analytical

methods can be used to estimate the equivalent length L_s . Figure 4.6 shows the deformed shape of the partially embedded pile in FEM-Design and the position of the equivalent length L_s that is predicted according to analytical methods for $L_u=6$ m.

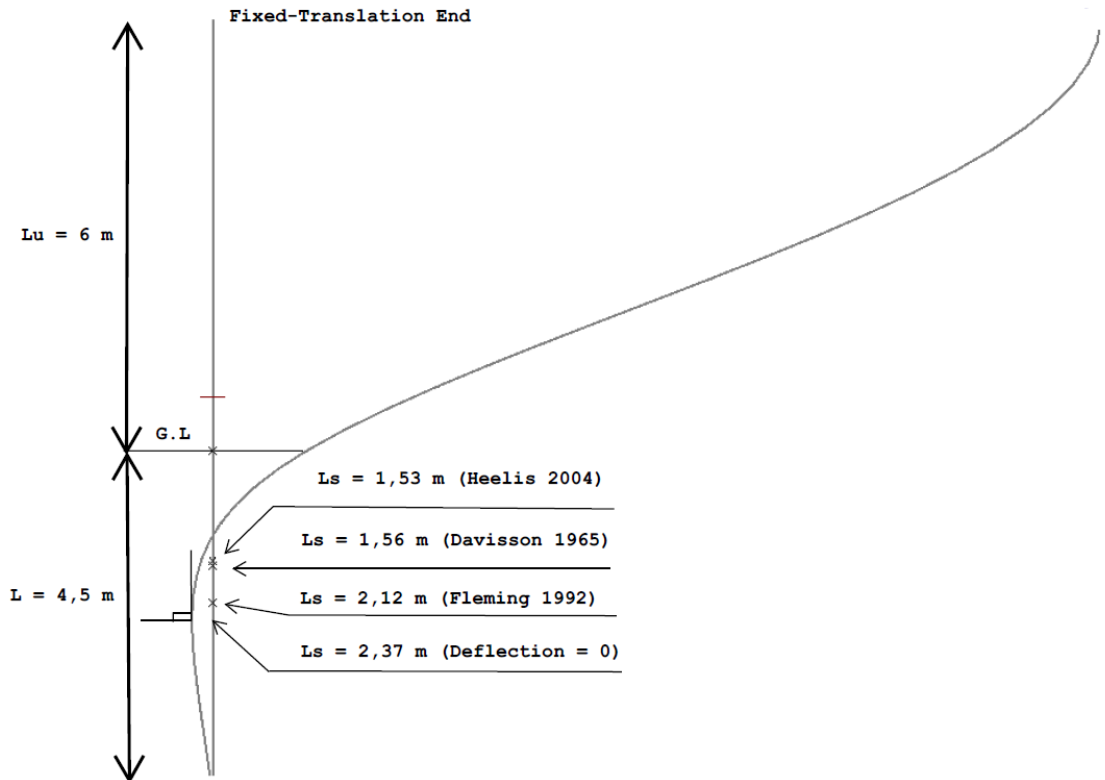


Figure 4.6: Deformed shape of the partially embedded pile in FEM-Design. G.L. is the ground level.

It can be noticed that the depth of the equivalent length according analytical methods is bounded between two points, the point where the deformed shape cross the pile and the point where the deflection is 0. These two points can be used to predict the depth of the equivalent length in an advanced problem. However to assume the depth where the deflection is 0 is a conservative estimation (on the safe side).

Conclusion

5.1 Conclusion

Case 1 with linear soil model shows that the total resistance of the pile model has lower ultimate load than the pile load test - even when K is increased. The pile model has in general a weaker behaviour than the pile load test. The modelling of the soil-pile interaction of the shaft consists of the supports with linear-elastic perfectly plastic behaviour. However, the plastic deformation cannot be obtained in the analyses due to the plastic limit (ultimate load) of each support.

Case 2 uses the over-consolidated soil model. Many of the soil input values are assumptions that have been converted from the Hardening Soil parameters. The support stiffnesses in FEM-Design are not stress-dependent for the over-consolidated soil model since they are generated independently on the vertical stresses. Instead, the soil-pile interaction is considered as linear elastic-perfectly plastic supports like the linear soil model, see Figure 3.9. The stiffness in over-consolidated model is stress-independent. It always considers the over-consolidated part M_0 in generating the stiffness. Hence, there is no difference between the linear and the over-consolidated model in generating the stiffnesses since they are generated independently of the effective stresses.

The lateral earth pressure coefficient K has been modified in both Case 1 and 2 to include the over-consolidation and to compare results. Though, the choice and modelling of the pile and soil in FEM-Design are too simplified compared with reality. FEM-Design does not include soil history or plastic deformation. The simplification is shown for the base, it only consists of one linear elastic-perfectly plastic support. One support is not sufficient to describe the real behaviour of the base.

The load-displacement curve is used to find the ultimate load and displacement for designing the pile. Therefore, it is important to plot a proper load-displacement curve in order to extract the ultimate load. FEM-Design does not match the real behaviour of the pile which makes it unsuitable to use for finding the ultimate load.

The buckling results of the FEM-Design and the three analytical methods have been predicted for a partially embedded pile. Here the critical length, the critical buckling load and the equivalent length have been found. FEM-Design results are close to the prediction of the two analytical methods, Davisson and Robinson (1965) and Heelis et al. (2004), while the results predicted in Fleming et al. (1992) are underestimated. This leads to conclude that FEM-Design is suitable for prediction of critical length, critical buckling load and equivalent length. The critical buckling load varies when

the unembedded length is changing, while the equivalent length of the embedded part of the pile is strongly influenced by the soil stiffness and pile stiffness but not by the unembedded length. The deformed shape which is the result from the stability analysis in FEM-Design can be used in order to predict the equivalent length L_s of the embedded part of the pile.

5.2 Recommendations for using FEM-Design

Strusoft specifies that the Pile feature in FEM-Design is a simple model for calculation of piles. FEM-Design can be used for internal stresses and displacement but not for capacity design. Though, the Pile feature is limited in practical use since it does only include a linear soil model and no consideration of soil history, stress-dependent stiffness or plastic deformations. Therefore, the behaviour until failure is simplified and does not fit the results of the load pile test for larger loads. There is no consideration of soil failure lines in the Pile feature and the results are independent on the width and depth of the soil. The software calculates the failure according to the sum of the shaft and base resistance but the total resistance is too small compared with the field measurement tests. FEM-Design chooses the lateral earth pressure coefficient, K , only based on the installation method, see Table 2.3. Though, the determination of K depends also on soil properties and soil history, which FEM-Design does not include. The user has to modify the K manually by recalculation of the plastic limits and inserting them in the pile properties. The user of the Pile feature need to have geotechnical experience to deal with the correct input values and the accuracy of the output results. The Pile feature considers only instantaneous calculations and no time-dependency or plastic deformation. Pile and settlement behaviour and water dissipation are highly dependent on time and plastic deformation in reality. Therefore, the real pile behaviour cannot be obtained in this software.

The user - an engineer - needs to stretch the pile to be in water and partly in soil to make the stiffnesses work correctly in the stability analysis. The modelling of the equivalent length gives reasonable results compared to the analytical methods. Therefore, FEM-Design can be used to estimate the critical buckling load of a pile. The partially embedded pile has a critical length L_c ; if the embedded length $L > L_c$, there will be no obtained increase in the critical buckling load.

FEM-Design does in certain cases illogical assumptions, which are not described in Strusoft (2016) or Szakály (2017). These are explained in Appendix A.

5.3 Recommendation for further studies

The only comparison of load-displacement behaviour between FEM-Design and load pile test is performed according to Wehnert and Vermeer (2004). This Thesis does not include other case studies which is a limited base to draw general conclusions of the software. It is recommended to compare the load-displacement behaviour of

FEM-Design with other field measurement tests. The validation of Wehnert and Vermeer (2004) has only been performed for drained soil conditions. A validation of undrained soil conditions will be relevant for further studies.

The verifications performed in the Thesis are related to fully and partially embedded piles at marine structures. FEM-Design has the ability to also do second order analyses and imperfection. These analyses are recommended to verify since these considerations are often relevant for pile design.

Bibliography

Alén, C.

2012. *Pile foundation - Short handbook (course material)*, 1.1 edition. Geotechnics – BOM045, Chalmers University of Technology, page 12.

Berre, S.

2017. Back calculation of measured settlements for an instrumented fill on soft clay. Master's thesis, Norwegian University of Science and Technology, Trondheim. page 35.

Davisson, M. T. and K. E. Robinson

1965. Bending and buckling of partially embedded piles. *International Conference on Soil Mechanics and Foundation Engineering*, 2. page 243-246.

Fellenius, B.

2018. *Basics of Foundation Design*, electronic edition. Pile Buck International. www.fellenius.net/.

Fleming, K., A. Weltman, M. Randolph, and K. Elson

1992. *Piling Engineering*, 2nd edition. Halsted Press. ISBN 0903384353.

Fleming, K., A. Weltman, M. Randolph, and K. Elson

2009. *Piling Engineering*, 3rd edition. Taylor and Francis. ISBN 0415266467.

Havel, F.

2004. *Creep in soft soil*. PhD thesis, Geotechnical division - Norwegian University of Science and Technology, Trondheim. URN:NBN:no-3497, page 33.

Heelis, M. E., M. N. Pavlovic, and R. P. West

2004. The analytical prediction of the buckling loads of fully and partially embedded piles. *Journal of Géotechnique*, 54(6).

Karstunen, M. and A. Amavasai

2017. Best soil: Soft soil modelling and parameter determination. Technical report, Chalmers University of Technology, Gothenburg. ISBN 978-91-984301-0-3, page 37.

Knappett, J. and R. Craig

2012. *Craig's Soil Mechanics*, 8th edition. Spon Press. ISBN 978-0-415-56125.

Lai, C.

2012. Port of long beach, wharf design criteria. Technical report, Port of Long Beach.

Meijer, K. and A. Åberg

2007. Krypsättningar i lera - en jämförelse mellan två beräkningsprogram. Master's thesis, Chalmers University of Technology. page 6.

NAVFAC

1986. *Foundation and Earth Structures*, 7.02 edition. Naval Facilities Engineering Command.

Olsson, M.

2010. Calculating long-term settlement in soft clays – with special focus on the gothenburg region. Technical report, Swedish Geotechnical Institute. page 35-36.

Parry, R. and C. Swain

1977. A study of skin friction on piles in stiff clay. *Ground Engineering*, 10(8). EMAP CONSTRUCT LIMITED, ISSN 0017-4653.

Skempton, A. W.

1959. Cast in-situ bored piles in london clay. *Géotechnique*, 9(4):page 153–173.

Strusoft

2016. *Geotechnical module in 3D*, 4.3 edition. download.strusoft.com/FEM-Design/inst170x.

Szakály, F.

2017. *Project plan of Simple pile feature*. Strusoft manual, download.strusoft.com/FEM-Design/inst170x.

Vesic, A.

1961. *Proceedings of the 5th International Conference of Soil Mechanics*. Dunod. page 845-850.

Wehnert, M.

2006. *Ein Beitrag zur drainierten und undrainierten Analyse in der Geotechnik*. PhD thesis, Universität Stuttgart. ISBN10 3-921837-53-7, page 22.

Wehnert, M. and P. Vermeer

2004. Numerical analysis of load tests on bored piles. Technical report, Institute for Geotechnical Engineering, University of Stuttgart. NUMOG, 9th.

Zhang, Q. Q., S. C. Li, F. Y. Liang, M. Yang, and Q. a. Zhang

2014. Simplified method for settlement prediction of single pile and pile group using a hyperbolic model. *Géotechnique*, 12(2).

Appendices

Appendix A: Guidelines for the software.

Appendix B: Calculation of stiffnesses and plastic limits in FEM-Design for Case 1.

Appendix C: Calculation of buckling capacities for Case 3.

Appendix A - Guidelines for the software

The following is the illogical input values and assumptions in FEM-Design which has been found during the work. These are not described in the manuals, Strusoft (2016) and Szakály (2017).

- The lateral earth pressure coefficient for bored piles in Table 2.3 is always chosen as $K=0.7$ in the software independent on the diameter of the pile.
- Table 2.4 shows the relevant value for determination of N_q . FEM-Design chooses always respectively the smallest or the largest value for friction angles below 26° or above 40° .
- FEM-Design calculates the relevant geometry data when a composite cross-section is created by the user. The software describes that the composite cross-section is based on the steel. The software does not include fully concrete cross-section for geometry data but does only include a small part.
- The existing tubular steel pipes in the cross-section library includes both the inner and outer circumferences for calculating the stiffnesses.
- The software assumes the fully pile length L in calculation of the stiffness K_x , see Equation (2.7), even though not the whole pile is located in the soil.
- The linear elastic analysis assumes the same base resistance for the pile in compression and tension, see also Section 2.4.1.
- The over-consolidated soil model for pile modelling does always choose M_0 when calculating the stiffnesses and does not use the other input parameters of the soil model. The over-consolidation model will always show the same output results as the linear soil model, see also Section 3.5.3.

Appendix B - Calculation of stiffnesses and plastic limits in FEM-Design for Case 1

The input values are found in Table 3.1

Pile:

$L := 9.5 \text{ m}$	Total length of pile
$E_p := 30 \text{ GPa}$	E-modulus of concrete C20/25
$D := 1.3 \text{ m}$	Diameter of the pile

$I_{p,z} := \frac{\pi}{64} \cdot D^4 = 0.14 \text{ m}^4$	Moment of inertia of the pile
--	-------------------------------

$r_0 := D \cdot 0.5 = 0.65 \text{ m}$	Radius of the pile
$P := \pi \cdot D = 4.084 \text{ m}$	Perimeter of cross-section

$A_{base} := \frac{\pi}{4} \cdot D^2 = 1.327 \text{ m}^2$	Area of the base
---	------------------

Soil:

$c_k := 20 \text{ kPa}$	Tertiary drained clay
$E_s := 0.06 \text{ GPa}$	E-modulus of the clay
$\mu_s := 0.3$	Poisson's ratio of the clay

$\gamma_{dry} := 20 \frac{\text{kN}}{\text{m}^3}$	Unitweights of clay
---	---------------------

$\gamma_{sat} := 20 \frac{\text{kN}}{\text{m}^3}$	
---	--

$\phi := 20 \text{ deg}$	Friction angle of the drained clay
--------------------------	------------------------------------

$N_q := 5$	For bored pile depending on friction angle, see Table 2.4
------------	---

$M_0 := \frac{E_s \cdot (1 - \mu_s)}{(1 + \mu_s) \cdot (1 - 2 \cdot \mu_s)} = 80769 \frac{\text{kN}}{\text{m}^2}$	Compression modulus of soil
---	-----------------------------

$G_s := \frac{E_s}{2 \cdot (1 + \mu_s)} = 23077 \frac{\text{kN}}{\text{m}^2}$	Shear modulus of soil
---	-----------------------

General:

$L_{element} := 0.5 \text{ m}$	Chosen division length
$L_{dry} := 3.5 \text{ m}$	Length of dry pile part
$L_{wet} := 9.5 \text{ m} - 3.5 \text{ m} = 6 \text{ m}$	Length of saturated pile part

$\gamma_w := 10 \frac{\text{kN}}{\text{m}^3}$	Unit-weight of the water
---	--------------------------

Lateral line motion springs K_z and K_y

$$k_{s,y}' := \frac{0.65 \cdot E_s}{D \cdot (1 - \mu_s^2)} \cdot \left(\frac{E_s \cdot D^4}{E_p \cdot I_{p,z}} \right)^{\frac{1}{12}} = 25249 \frac{kN}{m^3}$$

$$K'_y := k_{s,y}' \cdot D = 32824 \frac{kN}{m^2}$$

Lateral line motion springs K_{x1}

$$G_{s,middle} := G_s = 23077 \text{ kPa}$$

$$G_{s,bottom} := G_s = 23077 \text{ kPa}$$

$$\rho_m := \frac{G_{s,middle}}{G_{s,bottom}} = 1$$

$$r_m := 2.5 \cdot L \cdot \rho_m \cdot (1 - \mu_s) = 16.63 \text{ m}$$

$$k_s := \frac{G_s}{r_0 \cdot \ln\left(\frac{r_m}{r_0}\right)} = 10952 \frac{kN}{m^3}$$

$$K_{x1}' := k_s \cdot P = 44729 \frac{kN}{m^2}$$

Vertical pile tip spring K_{x2}

$$K_{x2}' := \frac{4 \cdot G_s \cdot r_0}{1 - \mu_s} = 85714 \frac{kN}{m}$$

Drained vertical plastic limit forces - line support

Compression

$$\delta := \phi = 20 \text{ deg}$$

Manually changed - FEM-Design chooses $\delta = \frac{3}{4} \cdot \phi$

$$K := 1$$

Manually changed - FEM-Design chooses $K = 0.7$

$$\beta := \tan(\delta) \cdot K = 0.364$$

$$L_{div.dry} := \frac{L_{dry}}{L_{element}} = 7$$

Numbers of stiffnesses for part of the pile

$$L_{div.wet} := \frac{L_{wet}}{L_{element}} = 12$$

$$\sigma_{v.dry}' := \gamma_{dry} \cdot L_{dry} \cdot 0.5 = 35 \frac{kN}{m^2}$$

$$\sigma_{v.wet}' := (\gamma_{sat} - \gamma_w) \cdot L_{wet} \cdot 0.5 = 30 \frac{kN}{m^2}$$

Calculation of plastic limits for each division:

Division 1 (dry): $n_1 := 1$

$$L_1 := L_{element} \cdot n_1 = 0.5 \text{ m}$$

$$L_{div.dry1} := \frac{L_{dry}}{L_1} = 7$$

$$P_{lim.x'line1} := \frac{\beta \cdot \sigma_{v.dry}' \cdot P}{L_{div.dry1}} = 7.432 \frac{kN}{m}$$

Division 2 (dry): $n_2 := 2$

$$L_2 := L_{element} \cdot n_2 = 1 \text{ m}$$

$$L_{div.dry2} := \frac{L_{dry}}{L_2} = 3.5$$

$$P_{dry.diff} := \frac{\beta \cdot \sigma_{v.dry}' \cdot P}{L_{div.dry2}} = 14.865 \frac{kN}{m}$$

$$P_{lim.x'line2} := P_{lim.x'line1} + P_{dry.diff} = 22.297 \frac{kN}{m}$$

Division 3 (dry):

$$P_{lim.x'line3} := P_{lim.x'line2} + P_{dry.diff} = 37.162 \frac{kN}{m}$$

Division 4 (dry):

$$P_{lim.x'line4} := P_{lim.x'line3} + P_{dry.diff} = 52.027 \frac{kN}{m}$$

Division 5 (dry):

$$P_{lim.x'line5} := P_{lim.x'line4} + P_{dry.diff} = 66.892 \frac{kN}{m}$$

Division 6 (dry):

$$P_{lim.x'line6} := P_{lim.x'line5} + P_{dry.diff} = 81.756 \frac{kN}{m}$$

Division 7 (dry):

$$P_{lim.x'line7} := P_{lim.x'line6} + P_{dry.diff} = 96.621 \frac{kN}{m}$$

Division 8 (dry/sat): $n_8 := 3$

$$L_8 := L_{element} \cdot n_8 = 1.5 \text{ m}$$

$$L_{div.wet8} := \frac{L_{wet}}{L_8} = 4$$

$$\frac{\beta \cdot \sigma_{v.wet}' \cdot P}{L_{div.wet8}} = 11.149 \frac{kN}{m}$$

$$P_{lim.x'line8} := P_{lim.x'line7} + \frac{\beta \cdot \sigma_{v.wet}' \cdot P}{L_{div.wet8}} = 107.77 \frac{kN}{m}$$

Div 8 increases with the average of difference in stresses for the dry and saturated conditions.

Division 9 (sat): $n_9 := 2$

$$L_9 := L_{element} \cdot n_9 = 1 \text{ m}$$

$$L_{div.wet9} := \frac{L_{wet}}{L_9} = 6$$

$$P_{wet.diff} := \frac{\beta \cdot \sigma_{v.wet}' \cdot P}{L_{div.wet9}} = 7.432 \frac{kN}{m}$$

$$P_{lim.x'line9} := P_{lim.x'line8} + P_{wet.diff} = 115.202 \frac{kN}{m}$$

Division 10 (sat):

$$P_{lim.x'line10} := P_{lim.x'line9} + P_{wet.diff} = 122.635 \frac{kN}{m}$$

Division 11 (sat):

$$P_{lim.x'line11} := P_{lim.x'line10} + P_{wet.diff} = 130.067 \frac{kN}{m}$$

Division 12 (sat):

$$P_{lim.x'line12} := P_{lim.x'line11} + P_{wet.diff} = 137.499 \frac{kN}{m}$$

Division 13 (sat):

$$P_{lim.x'line13} := P_{lim.x'line12} + P_{wet.diff} = 144.932 \frac{kN}{m}$$

Division 14 (sat):

$$P_{lim.x'line14} := P_{lim.x'line13} + P_{wet.diff} = 152.364 \frac{kN}{m}$$

Division 15 (sat):

$$P_{lim.x'line15} := P_{lim.x'line14} + P_{wet.diff} = 159.797 \frac{kN}{m}$$

Division 16 (sat):

$$P_{lim.x'line16} := P_{lim.x'line15} + P_{wet.diff} = 167.229 \frac{kN}{m}$$

Division 17 (sat):

$$P_{lim.x'line17} := P_{lim.x'line16} + P_{wet.diff} = 174.661 \frac{kN}{m}$$

Division 18 (sat):

$$P_{lim.x'line18} := P_{lim.x'line17} + P_{wet.diff} = 182.094 \frac{kN}{m}$$

Division 19 (sat):

$$P_{lim.x'line19} := P_{lim.x'line18} + P_{wet.diff} = 189.526 \frac{kN}{m}$$

Drained vertical plastic limit forces - point support

$$\sigma_{v.nom}' := \gamma_{dry} L_{dry} + (L - 3.5 \text{ m}) \cdot (\gamma_{sat} - \gamma_w) = 130 \frac{kN}{m^2}$$

$$N_c := (N_q - 1) \cdot \cot(\phi) = 10.99$$

$$P_{lim.x'.point} := A_{base} \cdot (\sigma_{v.nom}' \cdot N_q + c_k \cdot N_c) = 1155 \text{ kN}$$

Calculation of total resistance for Case 1:

$$R_{s.tot} = \Sigma P_{lim.x'line}$$

$$R_{s.tot} = 1074 \text{ kN}$$

$$R_b := P_{lim.x'.point} = 1155 \text{ kN}$$

$$R := R_b + R_{s.tot} = 2228 \text{ kN}$$

Appendix C - Calculation of buckling capacities for Case 3

Definition of values:

L_U	Free unembedded length
L	Fully embedded length
L_E	Total equivalent length
$L_{s'}$	Equivalent length of the embedded length
L_c	Critical length beyond it the pile behaves as if it was infinitely long
E_p	Pile stiffness
I	Moment of inertia of the hollow pile
E_s	Soil stiffness
A	Cross-section area of pile
A_{gr}	Cross-section area of the steel netto area
t	Thickness of steel
D_{out}	Diameter of pile
D_{in}	Inner diameter of pile
R	Non-dimensional parameter
k_s	Stiffness of the soil
K	End condition

Input values - Hollow steel pile:

$D_{out} := 323.9 \text{ mm}$	Standard geometry of pile
$t := 16 \text{ mm}$	
$E_p := 210 \text{ GPa}$	
$K := 1$	Based on end condition - fixed translation

Input values - Soil:

$k_{s,FEM} := 30533 \frac{\text{kN}}{\text{m}^2}$	Taken from FEM-Design
---	-----------------------

General calculations:

$$r := \frac{D_{out}}{2} = 162 \text{ mm}$$

$$D_{in} := D_{out} - 2 \cdot t = 292 \text{ mm}$$

$$A := \pi \cdot \left(\left(\frac{D_{out}}{2} \right)^2 - \left(\frac{D_{in}}{2} \right)^2 \right) = 15477 \text{ mm}^2$$

$$P := 2 \cdot \pi \cdot \left(\frac{D_{out}}{2} - \frac{0}{2} \right) = 1018 \text{ mm}$$

$$I := \frac{\pi}{4} \cdot \left(\left(\frac{D_{out}}{2} \right)^4 - \left(\frac{D_{in}}{2} \right)^4 \right) = (1.839 \cdot 10^8) \text{ mm}^4$$

Of a hollow circular steel pile

Calculation of analytical methods:

Davisson 1963

$$R := \sqrt[4]{\frac{E_p \cdot I}{k_{s.FEM}}} = 1.06 \text{ m}$$

$$L_U := 10 \cdot m$$

$$L := 4.25 \cdot m$$

$$L_{max} := \frac{L}{R} = 4.008 > 4.0 \text{ /OK to use Davisson}$$

$$L_{tot} := L_U + L = 14.25 \text{ m}$$

$$J_{R.Dav} := \frac{L_U}{R} = 9.43$$

$$S_{R.Dav} := 1.45 \quad \text{From Figure 4.3}$$

$$L_{s'.Dav} := S_{R.Dav} \cdot R = 1.538 \text{ m}$$

$$P_{cr.Dav} := \frac{\pi^2 \cdot E_p \cdot I}{K \cdot (S_{R.Dav} + J_{R.Dav})^2 \cdot R^2} = 2863 \text{ kN}$$

Heelis 2004

$$J_{R.Hee} := \frac{L_U}{R} = 9.43$$

$$\delta_H := \frac{L}{L_{tot}} = 0.298$$

$$S_{R.Hee} := 1.44 \quad \text{From Figure 4.3}$$

$$L_{s'.Hee} := S_{R.Hee} \cdot R = 1.527 \text{ m}$$

$$P_{cr.Hee} := \frac{\pi^2 \cdot E_p \cdot I}{K \cdot (S_{R.Hee} + J_{R.Hee})^2 \cdot R^2} = 2869 \text{ kN}$$

Fleming 1992

$$L_E := 2 \left(\frac{E_p \cdot I}{k_{s,FEM}} \right)^{0.25} = 2.121 \text{ m}$$

$$L_c := 2 \cdot L_E = 4.242 \text{ m}$$

$$P_{cr,Fle} := \frac{\pi^2 \cdot E_p \cdot I}{K \cdot (L_U + L_E)^2} = 2594 \text{ kN}$$

FEM-Design

$$\kappa_{CR} := 2.859 \quad \text{Critical parameter}$$

$$P_{actual} := 1000 \text{ kN}$$

$$P_{cr} := \kappa_{CR} \cdot P_{actual} = 2859 \text{ kN}$$